

*Engineering 90*  
*Senior Design Project*

*Design and Implementation*  
*of a Hybrid Electric Bike*

*Group Members: Muhsin Abdur-Rahman, Bo Hu*  
*Advisors: Erik Cheever, Fred Orthlieb, Mr. Grant Smith*  
*Date: May 05, 2005*

**Abstract:**

This paper describes the process of planning, designing, and testing a hybrid electric bicycle. It provides a lot of detail into the challenges of modifying an existing mechanical system to one that is based on both human propulsion as well as a set of electro-mechanical interfaces that provide assists. Through designing an electro-mechanical system, with various non-human inputs and feedback channels, a major challenge was centralizing the control of the system. After establishing criteria for speed, control, efficiency, and weight, we began a process of selecting parts and developing models for how the overall system including the rider could be integrated in a way that is both safe, and easy to use.

## Table of Contents

---

<u>Section Number</u>	<u>Page</u>
<b>Part I. Introduction</b>	
1.1 Background -----	1
1.2 Project Goals-----	1
<b>Part II. Mechanical Design and System Integration</b>	
2.1 Design Targets-----	2
2.2 Benefits of stage power transmission -----	2
<b>Part III. Motor Characterization &amp; Selection of Power Transmission</b>	
3.1 Overview-----	3
3.2 Acceleration Requirements -----	4
3.3 Gradient Ascent Requirements -----	4
3.4 Motor Selection -----	5
3.5 Selecting Speed and Gear Reduction -----	7
3.6 Battery Selection -----	7
3.7 Dynamic Torque Calculation -----	8
3.8 Deriving the Torque Constant -----	8
3.9 Motor Starting Current -----	11
3.10 Maximum Torque Calculation -----	13
3.11 Starting Torque for Bike -----	13
3.12 Voltage Speed Relationship -----	14
3.13 Motor Back-Emf Constant -----	15
3.14 Back-Emf & Electric Regeneration-----	16
<b>Part IV. Power Transmission &amp; System Integration</b>	
4.1 Clutch Performance Targets -----	18
4.2 Primary Stage of Transmission System-----	20
4.3 Transmission Intermediate Stage-----	21
4.4 Secondary Transmission Stage -----	22
<b>Part V. Mounting System</b>	
5.1 Section Overview -----	23
5.2 Battery Mounts -----	24
5.3 Motor Base Plate -----	26
5.4 Pillow Block Bearing Mounting Plate-----	27
5.5 Jackshaft Mounting Blocks-----	28
5.6 Motor Mount Plate -----	29
5.7 Modifying the Sprocket-----	30
<b>Part VI. Electrical System Design</b>	
6.1 Overview -----	30
6.2 PIC Selection -----	30
6.3 Throttle Input & PWM Speed Control -----	31
<b>Part VII. Circuit Design &amp; Implementation</b>	
7.1 Overview -----	33

7.2 Main Controller -----	33
7.3 Gate Driver Selection-----	35
7.4 Half-Bridge Circuit Function-----	37
7.5 Testing Regeneration Model & Control Circuit-----	42
7.6 Implications of Regeneration for Entire System-----	45
7.7 Problems with Using the IR2184 -----	45
7.8 Power & Safety Circuitry -----	47

**Part VIII. Feedback Features & System Integration**

8.1 Overview-----	49
8.2 Brake and Toggle Switch-----	49
8.3 Speed Sensor-----	49
8.4 Temperature Sensor -----	51
8.5 Current Sensor -----	53
8.6 Other Feedback components-----	54

**Part IX. PCB Design and Implementation in Multisim 7.0 and Ultiboard 7.0**

9.1 Electrical Design Criteria-----	54
9.2 Circuit Fabrication -----	59

Part X. System Integration & Conclusion-----	60
--	----

**References**

**Appendices**

## List of Figures

<b>Table 1: Power requirements for various accelerations</b>	<b>pg 4</b>
<b>Table 3: Hill-Climbing Power Requirements</b>	<b>pg 5</b>
<b>Table 4: Operating Voltage and Current during startup and continuous motor operation</b>	<b>pg 12</b>
<b>Table 1:IR2184 Pinout and Function</b>	<b>pg 36</b>
<b>Table 6: Circuit States and Functions</b>	<b>pg 39</b>
<b>Table 7: Modes of Circuit Operation as a Function of the Duty Cycle</b>	<b>pg 40</b>
<b>Table 8: System Analogs</b>	<b>pg 42</b>
<b>Figure1: Model of Hill-climbing</b>	<b>pg 5</b>
<b>Figure 2: Rad2GO 24VDC Motor</b>	<b>pg 7</b>
<b>Figure 3: Current Vs. Torque Graph</b>	<b>pg 11</b>
<b>Figure 4: Speed Constant from Motor Tests</b>	<b>pg 14</b>
<b>Figure 5: Back Emf Constant Derivation</b>	<b>pg 16</b>
<b>Figure 6: Regeneration Requirements</b>	<b>pg 17</b>
<b>Figure 7: Battery Mount Top Plate</b>	<b>pg 24</b>
<b>Figure 8: Battery Mount Bottom Plate</b>	<b>pg 25</b>
<b>Figure 9: Motor Base Plate (bottom)</b>	<b>pg 26</b>
<b>Figure 10: Motor Base Plate (top)</b>	<b>pg 26</b>
<b>Figure 11: Pillow Block Bearing Mounting Plate</b>	<b>pg 27</b>
<b>Figure 12: Jackshaft Mounting Blocks</b>	<b>pg 28</b>
<b>Figure 15: Motor Mount Plate</b>	<b>pg 29</b>
<b>Figure 16: Electronic Control Circuit</b>	<b>pg 31</b>
<b>Figure 17: Motor Control Circuit</b>	<b>pg 31</b>
<b>Figure 18: PWM Signal</b>	<b>pg 33</b>
<b>Figure 19: IR3709 Hex Power Mosfet</b>	<b>pg 34</b>
<b>Figure 20: IR2184 Gate Driver Typical Application</b>	<b>pg 35</b>
<b>Figure 21: IR2184 Gate Driver Implementation</b>	<b>pg 35</b>
<b>Figure 22: Input/Output Timing and Switching Waveforms</b>	<b>pg 36</b>
<b>Figure 23: Gate Driver used to Control the Clutch</b>	<b>pg 37</b>
<b>Figure 24: Motor Control through Half-Bridge Circuit</b>	<b>pg 38</b>
<b>Figure 25: Motor Simplification</b>	<b>pg 38</b>
<b>Figure 26: Battery Current as a Function of the Duty Cycle</b>	<b>pg 41</b>
<b>Figure 27: Test Setup for Forward Drive and Regeneration</b>	<b>pg 42</b>
<b>Figure 28: Coupled Motor Loaded at 7.5 Volts</b>	<b>pg 43</b>
<b>Figure 29: Coupled Motor Loaded at 9.5 Volts</b>	<b>pg 44</b>
<b>Figure 30: Coupled Motor Loaded at 12 Volts</b>	<b>pg 44</b>
<b>Figure 31: Circuit Isolation Components</b>	<b>pg 48</b>
<b>Figure 32: Speed Sensing Circuit</b>	<b>pg 50</b>
<b>Figure 33: TMPO1 Temperature Controller</b>	<b>pg 52</b>
<b>Figure 34: Final PCB Layout in Ultiboard 7.0</b>	<b>pg 58</b>
<b>Figure 35: Complete System Diagram</b>	<b>pg 60</b>

**Acknowledgements:**

We would like to thank our advisors, Dr. Erik Cheever and Dr. Fred Orthlieb, for their support, guidance, and encouragement throughout the project. From simple to complex problems that seemed impossible to solve, our advisors were always able to provide sound advice and often an elegant solution for chaotic combinations of problems.

We would also like to thank our machinist, Mr. Grant Smith for his assistance in designing and machining a number of the parts used in our system, as well as his patience with us as we used the machine shop. In addition, we would like to thank Edmund Jaodi, the college's electronics specialist, for his advice in selecting parts and assistance with mounting a number of the more sensitive electronic parts we used for our project.

We extend additional thanks to the product and plant engineers at both Gates Corporation as well as Warner Electric Corporation. Dick Hall of Warner Electric worked with us in selecting an electromagnetic clutch for the system, and donated the clutch for use in our project. Lastly Greg Ahlers, Stephen Johnson, and Levi Cambell assisted us in selecting the timing belt drive components, and also contributed the parts at no charge.

To all those who contributed to this project, but who are excluded from the list, we extend warm thanks to you as well. The combination of your collective support made the project all the more worthwhile.

## **Part I: Introduction**

### Section 1.1 Background

The system we designed is a hybrid electric bike. The project has a number of benefits to both the team members as well as external benefits through increasing awareness of alternative transportation modes. Despite the environmental friendliness of the project or the projected benefits of more people relying on non-polluting modes of transport, the main reason we selected the project was for the level of interaction between us, the engineers, and our product. Designing a transportation vehicle requires consideration of mechanical objectives, electrical objectives, safety criteria, comfort, user friendliness as well as an array of other objectives which may conflict under various circumstances. We hoped that through navigating our way through this vast set of criteria the satisfaction of completing the project would be much greater than other projects we could have selected.

Namely, we chose this project for the challenge of designing a mechanical system and implementing electronic control to dictate the response and performance of the system. The project seemed appropriate after having taken control theory and other courses that focused on design and feedback systems. Since, we have never had to design a complete electro-mechanical system of this magnitude; the project presented an interesting challenge. What made it even more challenging was the challenge of adapting an existing system to a set of criteria we determined.

### Section 1.2 Project Goals

The goals of the project were to design and integrate an additional power transmission drive an existing mechanical bike. We projected that we would be able to control the systems synchronously through electronic control interfaces. Our project focus was primarily to design a system capable of forward drive and electrical regeneration. Some additional goals or constraints to the project included the following: (1) limiting the costs of the system, (2) limiting the additional weight of the added drive and related components, (3) maintaining ease of operation of the bike when the electrical system is disengaged, (4) and integrating some of the mechanical features of the original system with those of the hybrid system.

We needed to select both the mechanical as well as electronic components fairly carefully to design a system capable of both forward drive and effective regeneration. The objective of saving costs was constrained somewhat by the limited time frame with which we had to complete the project. Although, we

could limit the additional weight as much as possible, we were constrained by the limitations of the existing bike frame.

The frame needed to be adapted to our application, but not at the expense of its structural integrity. As a result, we were advised by bike dealers to not drill into the frame to create mounting locations for the new power transmission and control components. Due to the existing frame being aluminum, we also could not weld to the frame. The combination of these structural constraints led us to developing other solutions for assembling the bike to reach our goals.

The last two of our goals were met by selecting the appropriate components for the system, but were not achieved without some loss of comfort to the rider. In a system so small, it is fairly difficult to achieve all the objectives without compromise.

## **Part II: Mechanical Design and System Integration**

### Section 2.1 Design Targets

The obvious goals of our system are to ensure efficiency of operation, and to meet the drive requirements. Given the types of sprockets available, the size of the motor we anticipated, safety concerns, and legal limits on the speed of motorized bikes, we determined that the maximum speed of the bike would be  $\approx 28mph$ . Given only these goals, the design would have been much easier.

An expanded set of goals included designing a system capable of regeneration, and to minimize the weight and size of components to maintain the character of a normal mechanical bike, when desired. Given the limitations of space, the design became much more difficult. The most critical of our objectives was to meet the forward drive requirements under a range of conditions (acceleration, hill-climbing, wet conditions). However, designing a system capable of regeneration determined the types of components we could use within our power-transmission system. Regeneration required that all the components be rigidly connected, so we could not use free-wheeling sprockets to reduce the effects of motor drag and maintain the character of a normal bike when the motor is turned off. We added another layer of complexity to the system by using an electromagnetic clutch to try and avoid the effects of motor drag.

### Section 2.2: Benefits of Two Stage Design

Essentially forward drive required only a motor and a set of sprockets to transmit the power from the motor to one of the wheels. Based on the available torque from the motor and the desired maximum

speed, we determined we would use a two-stage reduction to minimize the size of the components in the system. By splitting the transmission into two stages the number of components increases as well as the overall system complexity. The advantage of a two-stage design is that the size of individual components decreases. This was more critical to our system, than minimizing the number of parts.

Compared to other drive options, however, the two stage design is much more efficient, e.g. friction roller based approach. The advantages of a friction roller approach are its easy implementation, and high torque transfer from the roller to the much larger rear wheel. Unfortunately, there is a lot of inefficiency in this type of system due to the frictional losses of the tire rubbing against the roller. Using a single stage chain drive would have been preferable, but given the desired speed of the system and our torque requirements, we were limited by space. To reach the appropriate gear reduction given our speed requirement, we were limited by the space between the rear wheel and the chain stay which does not allow for a gear reduction greater than 3 (driven) or 4 (driven) to 1 (drive) using standard chain/belt sprockets. The two stage drive added to the complexity of the system, but provided a more elegant solution than the friction roller approach and a much more efficient solution.

The two stage design is also compatible with our goal of enabling regeneration, but also creating an efficient hybrid-electric solution. The two stage design enabled us to use a clutch in the system which would not have been possible in either the single stage or roller based drive system given our space constraints. The purpose of the clutch is to enable the rider to disengage the motor from the system during motor-less riding. By having a second stage, we created an appropriate mounting location for the clutch

### **Part III: Motor Characterization & Power Transmission Selection**

#### Section 3.1 Overview

This section of the paper deals with the mechanical design of the system and the various parts used in the system integration. The power transmission system consists of the motor, timing belt drive components, the clutch assembly, the chain sprockets and the rear wheel. However, before we could select these components, we performed some basic calculations relating energy transfer through the system. Primarily we focused on the current requirements of the system, and a number of torque-speed relationships. Both the acceleration on flat ground and hill climbing ability of the system depend on how much torque can be delivered by the various system components. Before we could size the motor and

batteries, we needed to estimate when the motor would demand the most current and the duration that it would draw its peak current. These situations would be at startup (acceleration) and when climbing a gradient. The main components affected by the following calculations are the motor and the battery. However, in order to maintain the order of the paper, we will focus on the motor, its characterization, and the subsequent power transmission components.

Section 3.2 Acceleration requirements

The external forces acting on the bike include drag due to the wind, the rolling resistance of the tires, and the force due to gravity. In order to expedite selection of the motor and the batteries, we neglected the drag forces acting on the system, and focused more on energy relationships, specifically the transfer of electrical energy into kinetic and potential energy.

In order for the bike to accelerate from a cold start, a sufficient amount of torque needed to be delivered by the motor and transmission components. As a result, we expected the motor to draw a large amount of current during the period of acceleration. We were able to approximate the amount of current required using the following set of energy relationships.

On flat terrain there is no change in potential energy which would cause the motor to need to deliver a counter torque to the force of gravity. As a result we only looked at kinetic energy for acceleration.

$$(1) \text{ Kinetic Energy} = \frac{1}{2} m \Delta V^2$$

**Equation 1:** (2)  $\text{Electrical Energy} = V \cdot I \cdot T$

$$(3) \text{ K.E.} = \text{Voltage rating motor} \cdot \text{Current required} \cdot \text{time to accelerate}$$

**Table 2: Power requirements for various accelerations**

Time to accelerate (s)	$\Delta$ Velocity	Voltage Available (V)	Mass	Current Required (amps)	Power Consumed (Watts)
20	25mph (11.2m/s)	24	260 Lbs (117.9 Kg)	15.4	369.6
40	25mph (11.2m/s)	24	260 Lbs (117.9 Kg)	7.7	184.8
60	25mph (11.2m/s)	24	260 Lbs (117.9 Kg)	5.1	122.4

Section 3.3 Gradient Ascent Requirements

**Equation 2**

$$gradient = \sin \theta = \frac{\Delta H}{\Delta x}$$

**Table 3: Hill Climbing Energy Requirements**

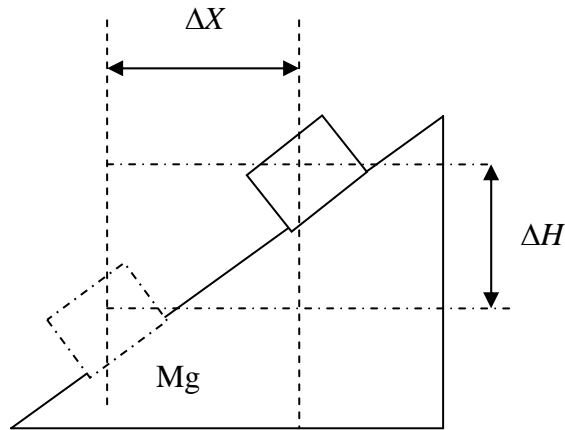


**Figure 1: Model of Hill-climbing**

Based on these calculations, it is clear that the system will draw the most current during hill climbing. Based on the suggestions of a number of electric bike and scooter dealers, we could use a 600 Watt motor to meet our system requirements. Given the terrain that the bike would normally be ridden on, these requirements would only be relevant over intermediate duties. Furthermore, a 600 Watt motor is more than sufficient for continuous operation.

Section 3.4 Motor Selection

Using the results from above, we selected a 600 Watt motor. Furthermore, we chose a Permanent magnet DC motor for the following reasons:

**Table 4: Hill-climbing power requirements**

Speed (Max)	Voltage Available (V)	Mass lbs (Kg)	% Gradient	Current (amps)	Power (Watts)
25 mph (11.2 m/s)	24	260 lbs (117.9 Kg)	5	27.3	655.2
25 mph (11.2 m/s)	24	260 lbs (117.9 Kg)	10	54.6	1310.4

1. Easy to control

2. Ability to function as a generator and regenerate power
3. Good torque-Speed relationships
4. High-power – weight ratio
5. Past experience through Control Theory
6. Ease of motor characterization (solving for torque constant, back-emf constant, voltage-speed constant)

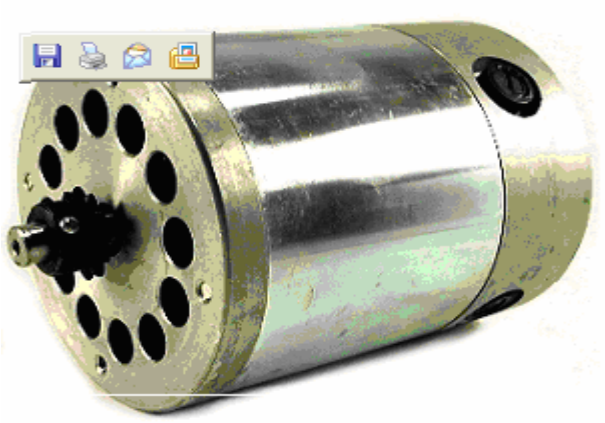
All of these reasons were critical for the project. Given the time constraint and the complexity of the other system components, a permanent magnet motor was ideal for our application. It would deliver adequate torque and rotate at a sufficient speed given several levels of gear reduction to improve the existing system. Another factor leading to our selecting a permanent magnet motor was its relative low costs compared to brushless motors, and the ease with which it could be integrated into the system.

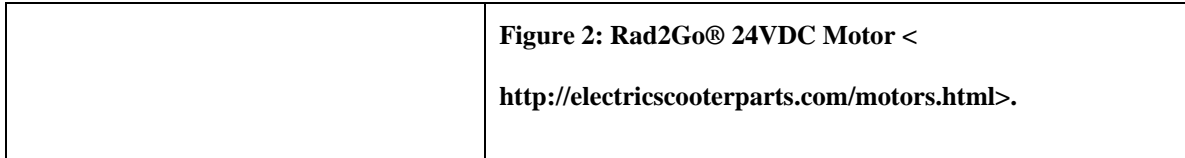
The next stage of the motor selection was to determine the voltage of the motor. This is important because the speed of the motor is a function of the system voltage. By choosing a higher voltage, the motor would also be capable of producing more power. By choosing an appropriate voltage we can limit the current draw of the motor. This is important for limiting heating but results in a loss of torque. For a permanent magnet motor there is a tradeoff between speed and torque by the following relationship.

### Equation 3: Torque-Speed Relationship

$$P = T \times RPM$$

We finally chose a 24 Volt motor. It is the most common selection for electric bikes and scooters, and was compatible with our goals for the system. The specific motor is described below.

<p>Actual Motor Specifications:</p> <ul style="list-style-type: none"> <li>● 600 Watt PMDC (Rad-2-go scooter) motor</li> <li>● 3100 RPM</li> <li>● 4.5 in x 5.5 in</li> <li>● 24 V x 25 Amp continuous rating</li> <li>● Peak ratings (intermittent duty)</li> </ul>	
--	--



Section 3.5 Selecting Speed and Gear reduction

Given our desired top speed of between 20 and 30 mph, we determined that we would design the overall system for a gear ratio from the motor shaft to the rear wheel of 1 (drive) : 9 (driven). The calculations were based on the following equations. The exact maximum speed we designed for is both a function of the motor we purchased as well as the sprocket sizes available at the dealers we chose to patron. We were constrained by an upper limit of 30 mph due to concerns about torque, and legal limits on licensing for motorized bicycles and scooters. The lower limit of 20 mph was not significantly influenced by outside variables except our desire to enhance the bike’s performance.

**Equation 4: Determining Bike Speed**

$$Speed_{motor} = \frac{3100 \text{ revolution}}{\text{minute}} * \frac{27p}{\text{revolution}} * \frac{60 \text{ minutes}}{1 \text{ hr}} * \frac{1 \text{ ft}}{12 \text{ inch}} * \frac{1 \text{ mi.}}{5280 \text{ ft}} = 249 \text{ mph}$$

$$\text{Desired Wheel Speed} = 27.7 \text{ mph}$$

$$\frac{Speed_{motor}}{\text{Desired wheel speed}} = \frac{249 \text{ mph}}{27.7 \text{ mph}} = 9$$

*Gear Reduction*

$$\text{Belt Drive} = N1 : N2 = 1 : 3$$

$$\text{Chain Drive} = N3 : N4 = 1 : 3$$

$$\text{Belt \& Chain Drive} = N1 : N4 = 1 : 9$$

Section 3.6 Battery Selection

When selecting batteries we were concerned primarily with cost, durability, energy density, and the number of recharge cycles. The most common solution for electric hybrid bikes is B&B batteries, specifically the EVP series, which are known for having a lot of recharge cycles. The most common batteries used are sealed lead acid batteries due to their low costs, and reasonably good energy density. These batteries are well suited to a hybrid electric application because they can be mounted in any orientation without the possibility of leakage or safety being compromised. After talking with an electric bike dealer, he advised us to select a battery with a higher rate of discharge, but also one with a high number of recharge cycles. Since we want to maximize the hill-climbing

and acceleration performance of our hybrid electric bike, we determined that the B&B High rate of discharge batteries would meet our needs. These batteries can be recharged over 200 cycles. For the amount of use the vehicle will likely have, this is more than sufficient.

We also wanted to extend the range of the vehicle, such that it is a viable mode of transport over medium distances, 30 miles or less. In order to meet this objective we needed a battery with a sufficient Amp-Hr Capacity. After surveying various electric bike designs, we observed that most used two 12-Volt batteries with Amp-Hr capacities varying between 8 Amp-hrs and 20 Amp-hrs. For our system we decided to purchase a 15-Amp-Hr battery. The costs does not increase dramatically as the Amp-Hr Capacity increases, however, the size of the batteries does. The B&B HR15-12 batteries would fit the scale of the system just as well as some of the smaller capacity batteries, which is why we selected it over some of the higher capacity batteries whose physical size increased beyond the system's scale.

Assuming the motor operates at its nominal continuous rating of 600 W, drawing 25 Amps, we can expect the 15 Amp-Hr batteries to deliver current for  $\approx 36$  minutes before needing to be recharged. Considering, the improbability of ever running the vehicle at its nominal rating for such a long period of time, the B&B HR15-12 Volt batteries were more than sufficient for use in the system.

#### **Part IV: Motor Characterization**

##### Section 3.7 Dynamic Torque Calculation

##### **Equation 5**

$$(1) \tau_{dynamic} = \frac{63000 \cdot HP}{RPM}$$

At a nominal power rating of 0.8 Hp, when the motor shaft rotates at 3100 rpm, the torque in in-lbs is 16.24 in-lbs. After a 3:1 gear reduction, the torque on the jackshaft is approximately 49 in-lbs. The final reduction results in a torque of 147 in-lbs. These calculations assume that each stage is 100 % efficient. Although, this is not the case, for the purposes of selecting components we carried the calculations and submitted the results to Warner Electric.

##### Section 3.8 Deriving the torque constant

The most important motor parameter in the design of the drive system was the torque constant. The following equation shows the proportional dependency of torque on current for a permanent magnet motor.

Solving for this parameter would enable us to determine the maximum torque available in the system, which we thought would significantly affect the selection of timing belt drive components and our selection of a clutch.

#### **Equation 6: Torque-Current relationship**

$$\tau = K_{\tau} I_{motor}, K_{\tau} \text{ is the torque constant.}$$

To find the torque constant,  $K_{\tau}$  (*in-lbs / Amp*), we needed to record the motors torque over a sufficient range of currents to observe an accurate linear relationship. To perform the tests we initially took advantage of the 12 point sprocket already set to the shaft of the motor by applying a torque wrench to the motor and proceeding to increase the current<sup>1</sup>. We soon found that the torque wrench was not sensitive enough for our application, as it measured torque in increments of 50 in-lbs. Upon finding that the torque wrench did not have a small enough breakdown of torque we set up a spring scale and proceeded to measure the force, lbs being applied to the end of a socket wrench. Because pictures were not taken during the actual experiment, we've included the procedure below to describe our test setup for the motor.

The exact procedure consisted of the following steps:

1. Clamp motor to prevent movement except for the rotation of the shaft.
2. Find a 12 point socket wrench and socket to attach to the existing 12-tooth sprocket riveted to the motor shaft.<sup>2</sup>
3. Measure distance from center of motor shaft to contact point of socket wrench and spring scale. (This is the moment arm)
4. Use spring scale with in-lbs sensitivity.
5. Record initial reading on spring scale<sup>3</sup>
6. Connect Kepco Power supply and motor in series through a terminal strip using 12 or lower gauge wire (must be rated > 20 Amps).

---

<sup>1</sup> Our electric power source was a Kepco power supply capable of outputting 40 volts and 30 Amps. The power supply was already available in the basement of Hicks. It had never been used, and as a result we needed to set it up for use. There was a manual available, and all the connections were on the back panel of the power supply.

<sup>2</sup> Adjust dial of socket wrench to allow free rotation in the same direction as the motor shaft rotates.

<sup>3</sup> This reading was subtracted as error due the spring scale not being zeroed.

7. Use Knife switches to disconnect motor from power supply if overheating occurs or in case of other undesired event.
8. If digital reading is desired, connect Ammeter between + terminal of power supply and the +terminal of the motor. (ammeter can only read up to 20 Amps, at which point a fuse blows)
9. Set Voltage limit on power supply to 24 Volts when circuit is still open.
10. Close the knife switches to complete the circuit.
11. Adjust current until dial moves on spring scale indicating presence of a force acting on the wrench.
12. Repeat step 9 for a series of currents up to current rating of motor (25 Amps).

After following this set of steps we solved for the torque using the following set of equations.

$$\text{Equation 7, } \begin{aligned} (1) \tau_{spring} &= F_{spring} \cdot r_{moment\ arm} \\ (2) F_{spring} &= K_{spring} x (\downarrow) \\ (3) \tau_{motor} &= \tau_{spring} \end{aligned}$$

The premise of this calculation is that the moments cancel each other out. As, the motor wanted to turn the shaft clockwise, CW, the spring force after being stretched tended to rotate the moment arm in the counterclockwise, CCW, direction. The spring applied just enough force to produce a torque sufficient to stop the rotation of the motor's shaft. Since at this point the system was in static equilibrium, we could equate the two torques as equal and opposites. Below is a graph of the torque (in-lbs) – current (Amps) relationship.

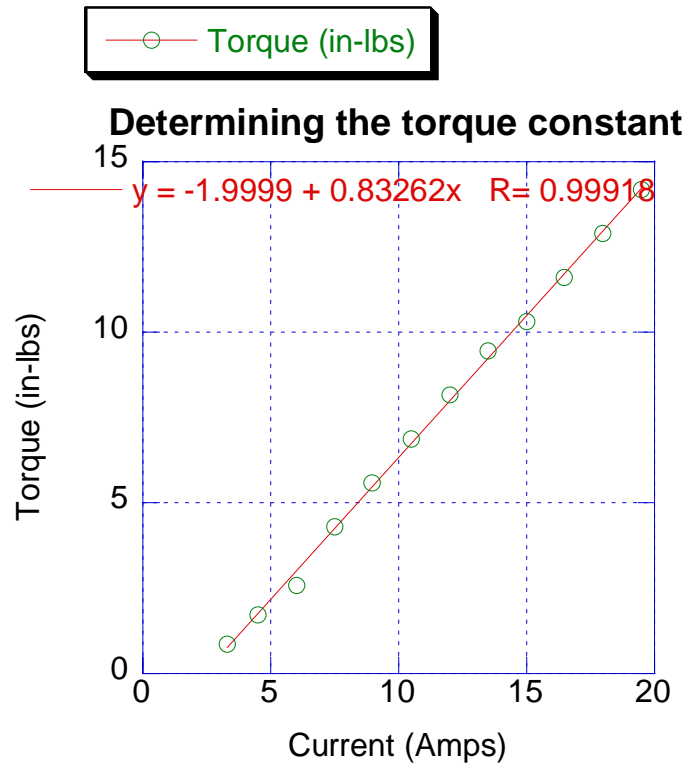


**Figure 3: Current vs. Torque graph**

The curve fit yielded  $K_t = 0.833 \text{ in} - \text{lbs} / \text{Amp}$ . It is worth noting that although the system was in static equilibrium during these tests, only a small amount of the motor's power was used. As a result, we did not have to worry about overheating or damaging the motor due to stalling. We used the torque constant in subsequent calculations to calculate the maximum torque available in the system.

Section 3.9 Motor starting current:

By finding the x-intercept of the graph you can find the amount of current needed to supply the motor before it starts to rotate the shaft in the direction determined by the polarity of the motor connections. The calculation led to a current of  $\approx 2.402 \text{ A}$ . This result is a fraction of what we measured in the lab. The actual current required to start the motor from a dead stop is  $\approx 3.44 \text{ Amps}$ . The required start-up current is partially explained by the effects of the inductance in the motor. Hence, inductors resist spontaneous changes in current.

The Y-intercept of the torque curve is negative because there is a negative mechanically induced moment exerted on the shaft. This torque is caused by the friction at the brushes and the sliding interaction between the brushes and the commutator. If you look at the back of the motor, you can see the brushes acting against the

commutator, which would produce a significant amount of friction. The current must be high enough to produce a torque to overcome opposing torque caused by moving components internal to the motor.

The combination of the negative mechanical and electrical torques contributes to the required current at startup being approximately 3.44 Amps to overcome the various resistive torques in the system.

**Table 5: Operating voltage and current during startup and continuous motor operation**

State	Voltage (V)	Current (Amps)
Dead-Stop	1.167	3.44
Continuous Operation (min)	0.541	1.05

In addition to contributing to the selection of the other power transmission components, we planned to use the torque constant, and other motor constants for closed loop control of the hybrid system. Specifically, the constants would enable us to determine the system plant (transfer function). Once we know the plant of the system, we should be able to implement a range of feedback (closed loop) control procedures which should give the bike better performance. All of the functions we would like to perform can be implemented using the microcontroller and various hardware components.

#### Section 3.10 Calculating Maximum torque

#### **Equation 8: Maximum Torque Calculation**

$$\tau_{\max} = K_{\tau} \cdot I_{\max}$$

To find the stall current we need to measure the resistance of the motor accurately. We do this based on measuring a series of resistances across the armature. In turning the shaft, we needed to ensure not to induce a current by turning too quickly. Hence the permanent magnets inside the motor could induce a current through the coil. To calculate the stall current, peak current, we need to adjust the armature angle in 45 degree increments. After taking the measurements we took an average and subtracted the offset, error measurement. Our results led to an average resistance calculation of 0.3 ohms. With a battery supply capable of producing 24 Volts, the stall current is 80 Amps according to ohms law<sup>4</sup>. This result is

---

<sup>4</sup> Ohms Law  $V = IR$

consistent with estimates we got from electric bike dealers. Based upon an average of the torque constant we found over several trials, the motor is capable of delivering a max torque equal to the following:

$$I_{\max} = 80 \text{ Amps}$$

$$K_{\tau, \text{avg}} \approx 0.8326$$

$$\tau_{\max} = K_{\tau, \text{avg}} \cdot I_{\max} = 66.61 \text{ Lb} \cdot \text{in} = 5.55 \text{ lb} \cdot \text{ft}$$

#### **Figure 4: Maximum torque calculation**

Note that with a 24 Volt power supply, the maximum power that can be delivered by the motor is

$$P = VI = 1920 \text{ Watts} = 2.57 \text{ Hp} .$$
 We would use this result in later sections, as it was critical in

determining what clutch and belt drives were compatible with our system.

#### Section 3.11 Starting torque for bike

In addition to the above tests, in coordination with two of the E14 students, we performed direct tests with the bike to measure the starting torque. Although, the data is not included in this report, we calculated the starting torque as 52 in-lbs. This experiment consisted of attaching spring scales to a pole and to the rear wheel of the bike. We then turned the pedal crank until the rear wheel turned slightly, and measured the force on the spring scale. The radius of the bike wheel was then multiplied by the spring force to calculate the torque. Although, this was a rough estimate of the starting torque, it is useful in assessing whether the motor would deliver adequate torque for the system. In addition, through the gear reduction of 9 to 1, theoretically, the motor would only need to deliver 1/9<sup>th</sup> of the calculated starting torque. As a result, the current requirements are much less significant for starting the bike.

#### Section 3.12 Voltage Speed Relationship

Permanent magnet DC motors' speed is proportional to the voltage you place across the motor terminals. The following equation describes this relationship.

#### **Equation 9**

$$V_{\text{supply}} = K_{\omega} \omega$$

Again, by graphing the angular speed of the motor as a function of the voltage we only need to calculate the slope to determine the proportional constant relating speed to voltage.

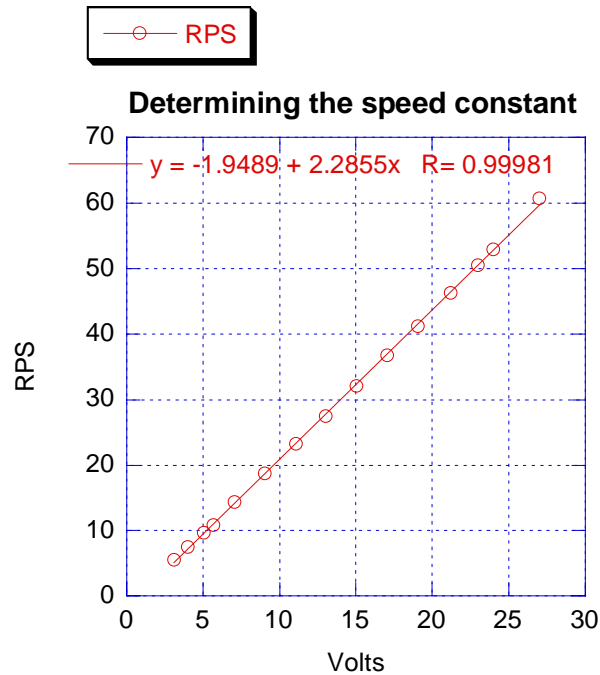


**Figure 5: Speed Constant from motor tests**

Using a linear curve fit of the graph we observed that for every volt from the power source, the motor would rotate 2.29 RPS.

Section 3.13 Motor Back Emf Constants

Given the motor's resistance of 0.3 ohms, the back emf constant can be solved for the motor. The equations of interest to us were the following.

**Equation 10**

$$(1) E_m = K_m \omega$$

$$(2) i_m = \frac{V_{Batt} - E_m}{R_m}$$

In the lab we collected data for the current through the motor, the voltage placed across the motor from the power supply, and the speed as measured by a contact/optical speed encoder provided by Prof. Cheever. The voltage observed is approximated by the difference of the back emf and the supply voltage. Equation 2 can be expanded to the following equation:

$$(3) i_m = \frac{V_{Batt}}{R_m} - \frac{K_m \omega}{R_m}$$

By dividing through by  $\omega$  we yield the following equation

$$(4) \frac{i_m}{\omega} = \frac{V_{Batt}}{\omega \cdot R_m} - \frac{K_m}{R_m}$$

And could then plot current per revolutions per seconds (rps) as a function of the voltage per rps.

The results were as follows.

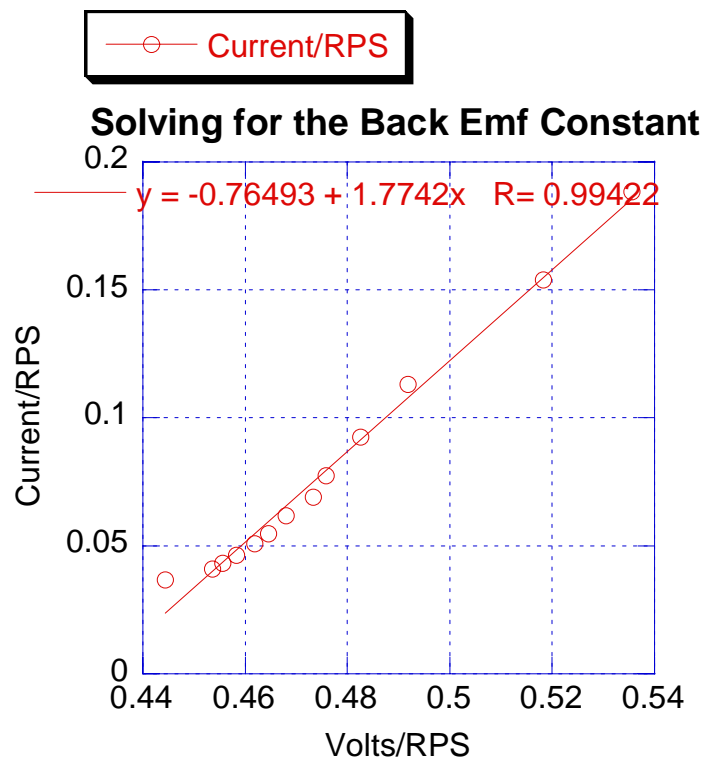


**Figure 6: Back Emf Constant Derivation**

After performing a linear curve fit we found that the equation that fit the line was

$$y = -0.76493 + 1.7742x \quad R = 0.99422$$

**Figure 7: Curve fit for solving for the back emf constant**

$\frac{K_m}{R_m} = 0.76493$ . Based on our measurement of  $R_m = 0.3 \Omega$ , we could easily solve for the back emf constant,

which is equal to  $0.2295 \frac{\text{Volts}}{\text{RPS}}$ . This means that at a top speed of 3100 rpm, the back emf produced is

11.86 Volts, and at half speed the back emf is 5.93 Volts.

#### Section 3.14 Back Emf of Motor and Electric Regeneration

The motor's back emf voltage is dependent upon the speed at which the motor turns. Furthermore, the speed at which the motor turns is dependent on the combination of mechanical energy via the pedals as well as electrical energy from the batteries. As the motor turns faster, the back emf increases. In order for regeneration to occur the motor shaft has to rotate at a faster rate than the (voltage across its terminals) \* (speed constant). This is why regeneration occurs when a rider goes down a hill. As the overall mechanical system is traveling at a fast rate the transmission system components translate the energy from the rear wheel to the motor, whether the supply voltage is on or off. For optimal regeneration to occur it is preferable that the supply voltage be as low as possible so that the back emf can exceed the battery voltage and force current to flow into the battery. Using the same data, we used to find the back-emf and speed constants, we can show that regeneration is much more likely to occur at lower voltages.

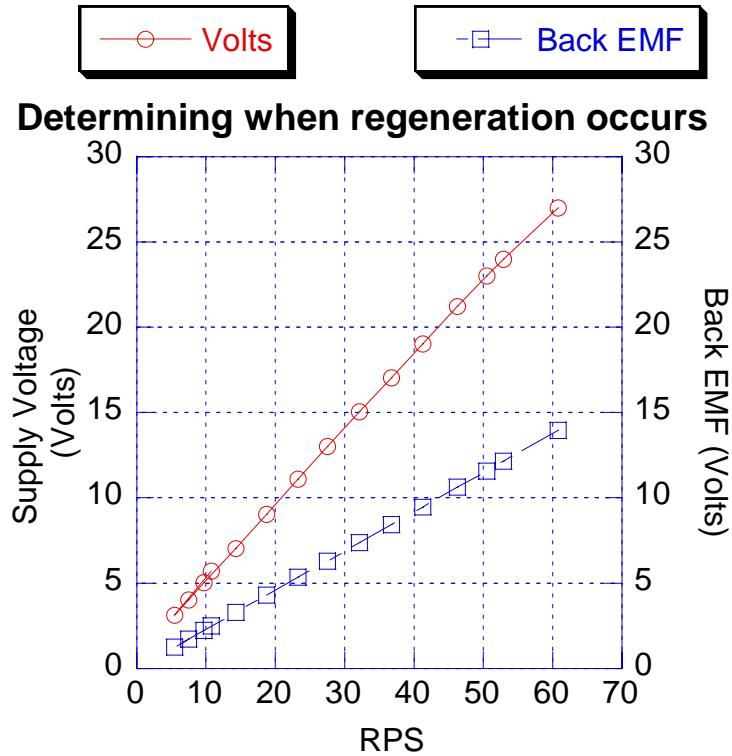


**Figure 8: Regeneration requirements**

As shown by the graph it is clear that regeneration is much more likely to occur at lower speeds. At the maximum speed recorded, 61 RPS, the back EMF is equal to 13.94 Volts and the supply voltage is approximately 27 volts. Given the supply voltage, for regeneration to occur at top speed, the actual speed of the motor would have to increase by the following.

**Equation 11:**

$$(1) \frac{V_{supply} - E_m}{K_m} = 57 \text{ RPS}$$

57 RPS is equivalent to 3414 RPM, which is more than double the motor's top speed. At the low input voltage, the motor speed would only have to increase by 5.54 RPS, which is equal to 332 RPM. It is significantly easier to achieve regeneration at the lower speed than to try to get regeneration at higher speeds.

#### **Part IV: Power Transmission & System Integration**

##### Section 4.1 Clutch Performance Targets

In selecting a clutch we inspected a number of clutch designs including a centrifugal clutch, and form-sprag clutch. Operationally, these were probably the simplest clutches to use since their actuation is automatic and does not require the rider to use a lever or switch mechanism. In the case of a centrifugal clutch, it engages once the input reaches a certain RPM. The problem with the centrifugal clutch is that it is not compatible with our goals of regeneration. Regeneration entails mechanical energy being stored as electrical energy, and requires the motor to act like a generator. A centrifugal clutch only connects the output to the input when the motor is spinning at a certain rate. Until the motor reaches the required rpm for engagement, the output is locked in place. Since all of the parts in the transmission system are connected rigidly, the rider would not be able to pedal unless the motor were turned on, which defeats our objective of maintaining the original character of the system.

An electromagnetic clutch was selected for both its simplicity of operation, as well as its functionality. The use of this clutch is to minimize parasitic losses during operation of the bike when the motor is off. The motor has the potential to create a lot of drag within the system such that the rider would experience discomfort when trying to pedal. In the same way as an operator of an automobile can disengage the clutch and transmission from the motor by applying pressure to a lever, we are able to disengage and engage the motor through an electric switch mechanism. As 12 volts is applied across the terminals of the clutch, a current flows through its field coil which creates a magnetic field. The lines of flux are then transferred through an air gap between the field and the rotor, and as the rotor is magnetized it attracts the armature which is a part of the output portion of the clutch, and includes the hub. The clutch engagement is essentially based on contact frictional forces, but is highly efficient with very good torque transfer characteristics. In the absence of a voltage across the clutch terminals, the input and output devices of the clutch are independent.

We chose an electric clutch primarily due to the ease with which it could be controlled. With limited space on the bike, and an uneven distribution of weight it did not seem reasonable to install a mechanical clutch which would require the rider to operate a lever in addition to the other control mechanisms on the bike. An electrical clutch could be integrated within our control circuitry, and would require very little input from the rider.

Our configuration consists of the motor and timing belt assembly connected through the output, whereas the jackshaft, small chain sprocket, and rear wheel assembly comprise the input assembly. The large timing belt is mounted over the hub of the clutch on the output. There were a number of other goals and features of the clutch that concerned us during selection. (See appendix for pictures)

The clutch needed to be able to transmit adequate torque and turn in the clockwise direction given it's placement in the system. The torque requirement was not hard to meet because our application is so small. Our motor is designed for continuous operation at fractional horsepower. Most of the clutches that were accessible to us were designed for much heavier systems requiring much higher torque delivery. The other requirement of clockwise rotation was also not a real issue. While there are a number of clutches that can rotate in either direction, most are designed up to a torque limit in either direction. After talking with a number of application engineers at Warner Electric Corporation, we concluded that this limitation was not applicable to our system, as the maximum torque required was much lower than the overrunning torque in either direction for the clutch we selected. Since the engagement is based on contact forces (friction), there may be a potential for slippage however, since the clutch is somewhat oversized for our system. However, until we perform testing, we will assume 100% efficiency and 100% torque transfer from the input to the output.

Electrically, we were concerned with the heat losses associated with the clutch. After looking at a number of clutch designs provided by Warner Electric we selected one with a low current requirement and low on resistance, that operated on a 12 Volt supply. As a result, we were able to meet our requirements of low-power dissipation relative to other clutches<sup>5</sup>.

The main problems with the clutch are its weight and size. Bikes are not designed for clutch installation, and thus, there were a limited number of locations to install it. We would have liked to install it such that its output shaft would be on the left side of the bike. Typically the motor would be the input, and the rest of the transmission system would be a part of the output system. However due to the location of the rear wheel chain sprocket, we could not use the clutch on the left side of the bike. It was more practical to install the clutch on the right side of the frame for the following reasons.

---

<sup>5</sup> I-5215-82 GT Clutch draws a current of 4.89 Amps with an on resistance of 2.45 ohms, resulting in a power loss of 58.59 Watts. The clutch we selected, I-5215-17 RMS Clutch/Brake draws a current of 1.67 Amps with an on-resistance of 7.18 ohms. The heat loss for our clutch is significantly less than the GT clutch we considered.

1. Clutch output offset: 1.857" from pillow block bearings
2. Pillow Block Bearings offset 0.625" from center line of frame
3. Sprocket offset 1.3" from center line of frame

Given these measurements, installing the clutch on the left side was simply not feasible. The two chain sprockets would have been badly misaligned. By installing the clutch on the right side we were able to achieve alignment of the small chain sprocket with the large chain sprocket bolted to the hub of the rear wheel. In addition, we decreased the overall weight of the system, since we could bore out (3.7") the large timing belt pulley to fit over the clutch face. Had we installed the clutch on the left side of the frame, it would have been necessary to design a plate to match the bolt holes on the face of the clutch and mount the small chain sprocket to the plate. The disadvantage of installing it on the right side is that the weight is disproportionately distributed on the right side of the bike. In addition to the clutch, the motor center is offset to the right side, as well as the large timing belt.

The two chain sprockets would have been misaligned, thus causing abnormal stresses on the chain which would result in damage and poor operation. The second preferred location would have been installing it directly to the motor shaft. This was not possible however because the shaft would not have given the proper engagement. These obstacles could not have been avoided given the budget of the project and the non-traditional use of the clutch. There are no custom designed components in the system, and as a result the design needed to compensate for the incompatibility of the various components.

#### Section 4.2 Primary stage of transmission system

According, to a number of electric bike hobbyists, timing belt drive is preferable to chain drive when the RPM exceeds 1000 rpm. Timing belts are significantly less noisy than chain at high rpms. At a top speed of 3100 rpm at the motor shaft, we determined that we would reduce the speed by 3 in the primary stage through appropriate selection of timing belts. The main factors which affected our selection were the maximum Hp calculation we performed earlier, the gear reduction from the motor to the jackshaft (intermediate shaft where the clutch and chain sprocket are mounted to), the center – center distance of the timing belts and a service factor<sup>6</sup> to ensure durability of the timing belts. Gates provides software titled

---

<sup>6</sup> A service factor is a multiplier applied to the horsepower which changes depending on the usage of the drive components. Since our system has relatively low torque requirements given the capacities of the drive components, the service factor used to design our timing belt drive was modest.

“Gates Design Flex II”, which enabled us to design the timing belt drive ourselves. Ultimately, however a plant engineer at Gates used the information we collected on the timing drive, and created a set of recommendations for us.

We considered additional factors such as the bore size of the timing belt drive components, and whether any of the parts could be modified to meet the systems needs. Specifically, we wanted a timing belt with a wide enough bore such that it could be mounted directly to the hub of the clutch after boring it out. Due to the clutch, the timing belt components are somewhat oversized. However, we were still able to avoid the pedal crank, and other critical parts of the existing bike frame where clearance is necessary.

The final drive was designed for an ideal center-center distance of 8.44”, HP of 3.9, and a speed down (gear reduction) of 3.05, between part #'s: (1) 8MX-22S-12 and (2) 8MX-67S-12. The middle number signifies the # of grooves in the timing belt, and determines the speed down ( $67/22 = 3.05$ ). The ideal center distance is different from the c-c distance we designed for but is not significantly different, only +65 thousandths. According to engineers at Gates Corporation, the poly chain timing belt drive we implemented is as efficient as a chain drive, if not more.

Originally Gates Corporation planned to provide the complete drive, both primary and secondary, but due to space constraints we could only implement the belt drive in the first stage. As a result, we had to select chain sprockets for the secondary system, as the width of the chain is much narrower than for a belt, which would aid us in aligning the chain drive.

#### Section 4.3 Transmission intermediate stage

The jackshaft represents the intermediate stage of the transmission system. It is simply a shaft which connects two stages of a power transmission (High speed-low torque & low speed – high torque). The shaft needs to be supported by bearings at each end of the drive. Therefore, one bearing would be near the small chain sprocket, and the other placed near to the clutch assembly. Due to the location of our jackshaft we determined that two pillow block bearings would be sufficient. The steel shaft is secured by 4 tap screws, two from each pillow block bearing. The shaft itself was a ½ “ dia. by 7.5” long. This allowed for the width, 1.5”x2, of two pillow block bearings, the clutch depth, 2.07”, and the seat tube width 1.5”.

In addition to the steel rod, we used for the jackshaft, we had “Smitty” make an aluminum sleeve with a 1” diameter to ensure proper engagement with the clutch input assembly. For proper engagement

the sleeve had a 1/4" keyway and extended 1.857" into the clutch assembly. To complete the installation, the steel rod was tapped for a 3/8" screw on the end extending into the clutch assembly. Later, we fastened a screw into the center of the steel rod, from the output side of the clutch. This fastener is used to keep the clutch assembled. The bolt needed to be torqued to approximately, the same torque as the maximum static torque specification for the clutch. In designing the sleeve for the steel rod, we needed to ensure that we leave sufficient space for the air gap. Had we not taken this precaution, we would have inhibited the rotor from becoming magnetized, and prevented engagement of the input/output systems. After completing this installation and bolting the timing belt to the face of the clutch, the primary drive stage was essentially complete.

#### Section 4.4 Secondary Transmission stage

The second stage of the transmission was significantly simpler than the primary stage, which included the clutch, the motor, and timing belt drive. Because of the standard usage of chain drives for this application, we did not go into as much detail in selecting the chain drive as we did for the selection of other parts. The main measurement required was the c-c distance from the jackshaft to the rear wheel hub center. We designed the second stage c-c distance as 14.125". The main consideration in selecting the chain sprockets is ensuring that the pitch is the same for the chain, and two sprockets.

Chain drives are generally much more efficient than belt drives when the center – center distance increases. The second stage consisted of only two chain sprockets, an 18 tooth sprocket and a 55 tooth sprocket to achieve a gear reduction of 3.06. In designing the secondary stage, we needed to first choose the type of chain, and chain sprockets we wanted to use. We observed a number of bike designs which used #35 chain. Most scooters however used #25 chains. The numbers refer to the pitch<sup>7</sup> of the chain. Consequently, #35 is much heavier than #25 chain. We were able to eliminate bike chain due to the lack of sprockets which could be mounted directly to the jackshaft. Scooter chain is half the pitch of bike chain and is also more flexible. For the size of our system, it seemed more practical to use #25 chain over #35 chain to avoid adding much more weight to the system. #25 chain is also much easier to install than #35 chain because it is smaller. By using #25 chain, we were also able to select smaller chain sprockets since the teeth are more closely spaced. This was important since the space between the chain-stay and bolt-disk

---

<sup>7</sup> Pitch is the distance between the chain links.

patter was very tight. Based on measurements of the bike frame, the driven chain sprocket could be no greater than 5" in diameter. Ultimately, we were forced to modify the sprocket such that it would fit over the hub's flange and be further displaced from the chain-stay despite its outer diameter of 4.5". This was because the chain did not clear the chain stay.

See appendix for timing belt design file:

## **Part V: Mounting system**

### Section 5.1 Overview

In order to minimize the additional weight to the system, most of the mounting plates and devices are made from 1/4" aluminum. The standard clearance holes were 17/64" and tapped holes, 1/4". The only bolts and mounting points that deviated from this convention were the water bottle clearance holes and the holes used to mount the pillow block bearings.

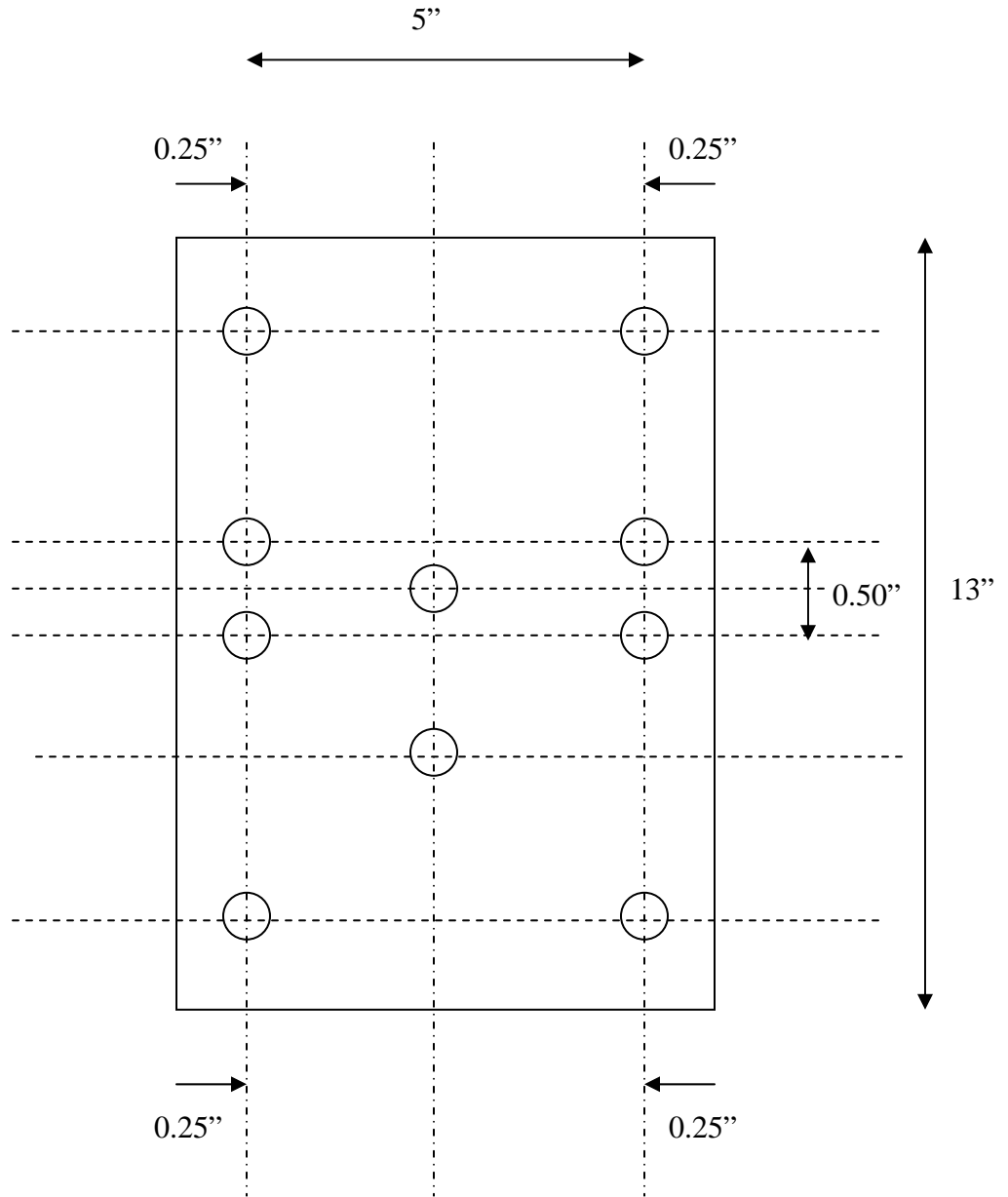
The order in which the mounts were made was the following:

- 1) Battery mount – 2 plates (13"x5"x0.25"), 1/4 " all-thread
- 2) Jackshaft mount – 3 plates
- 3) Motor mount – 3 plates
- 4) Controller Box

In this section we give a brief description of all the mounting components with basic installation details.

Section 5.2 Battery Mounts

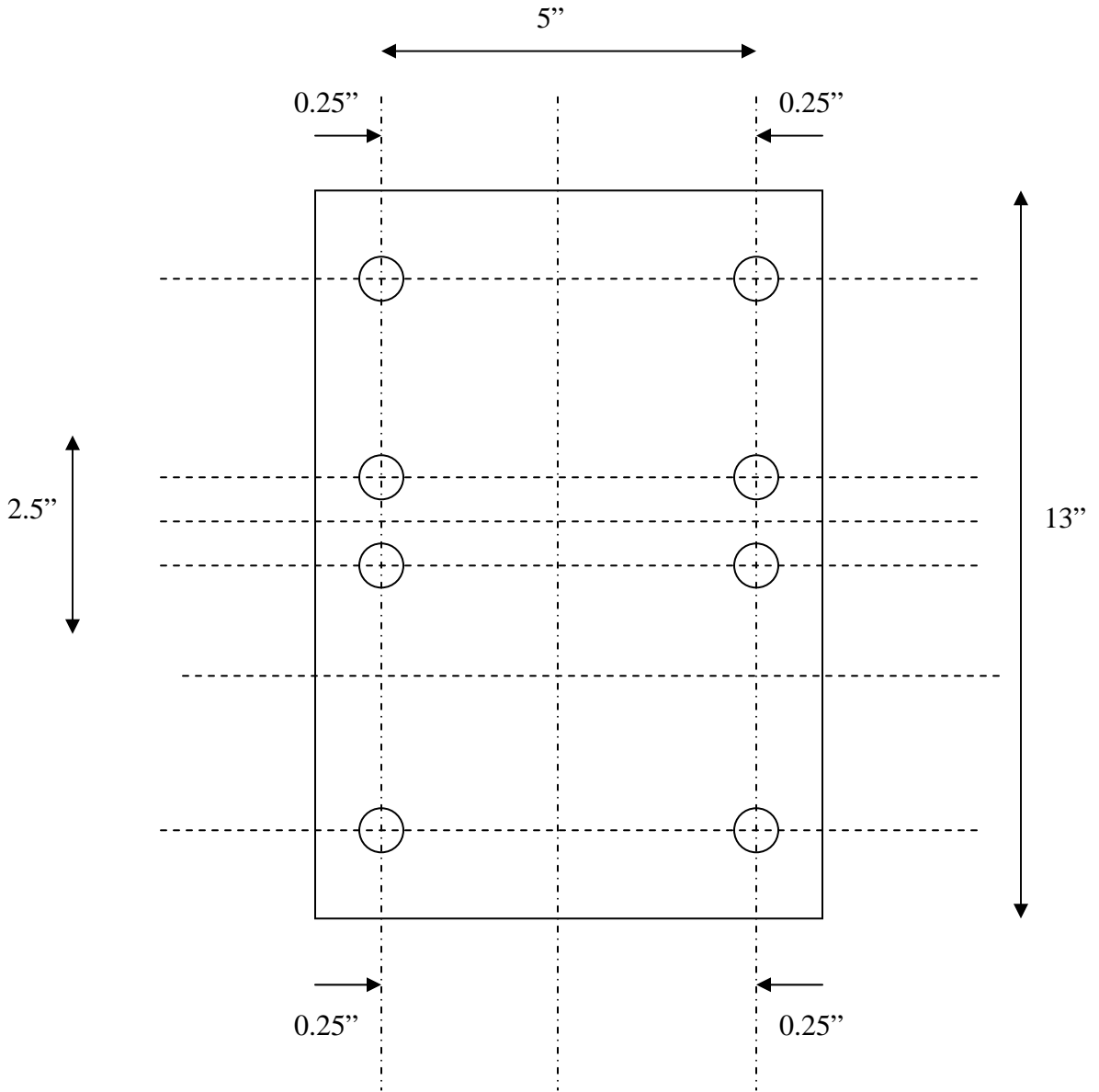
Mount Type: Base (top plate)  
 Clamp Material: 1/4" All thread



Hole Placement	Screw Size	Type	Drill type
Periphery	1/4"	Clearance	17/64"
Interior	10-32	Clearance	#21

Battery Mounts: Bottom Plate

Mount Type: Clamp  
 Clamp Material: 1/4" All thread

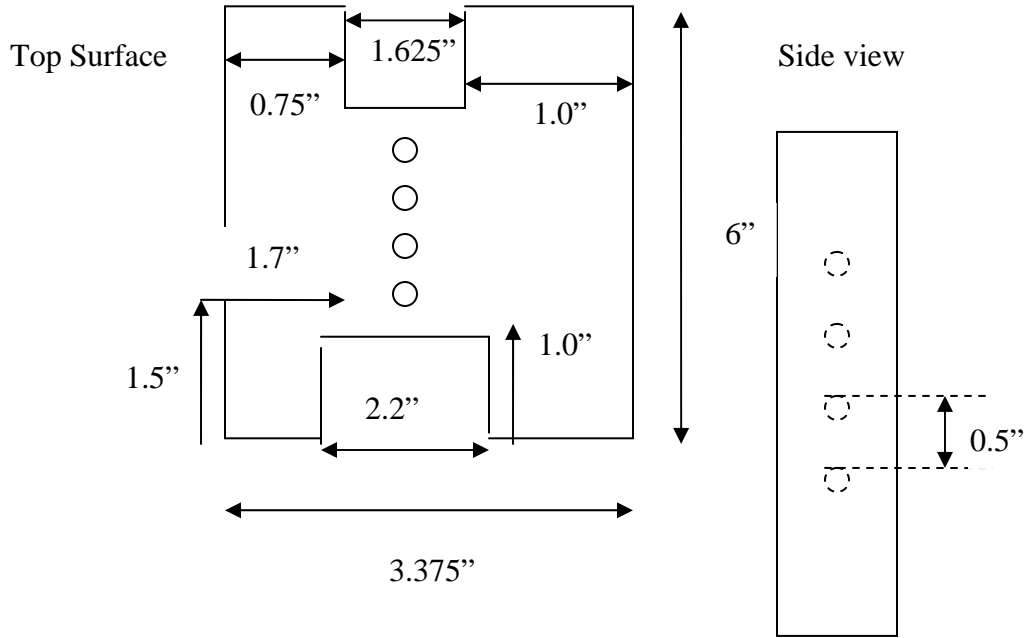


Hole Placement	Screw Size	Type	Drill type
Periphery	1/4"	Clearance	17/64"

The following are the set of motor plates used to install the motor. The top plate is the base plate for the motor mount and the bottom plate is used as a clamp to provide more support to the motor assembly.

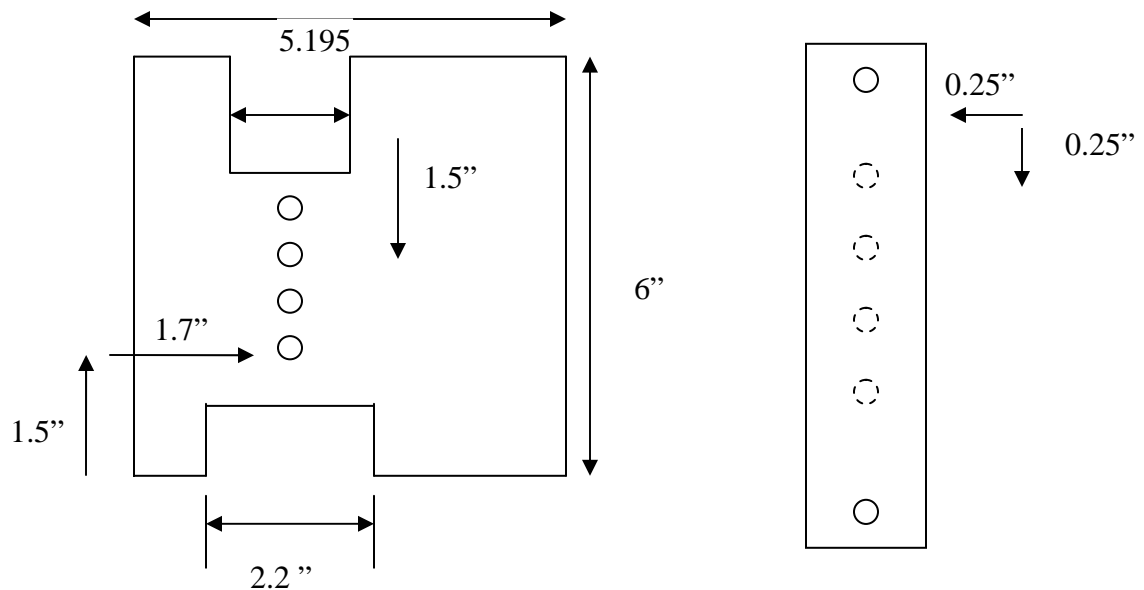
Part	screw size	Drill Tap
Top Plate	1/4"	17/64
Bottom Plate	1/4"	17/64

Section 5.3 Motor Base Plate



Top Motor Base Plate

Side View 1 & 2

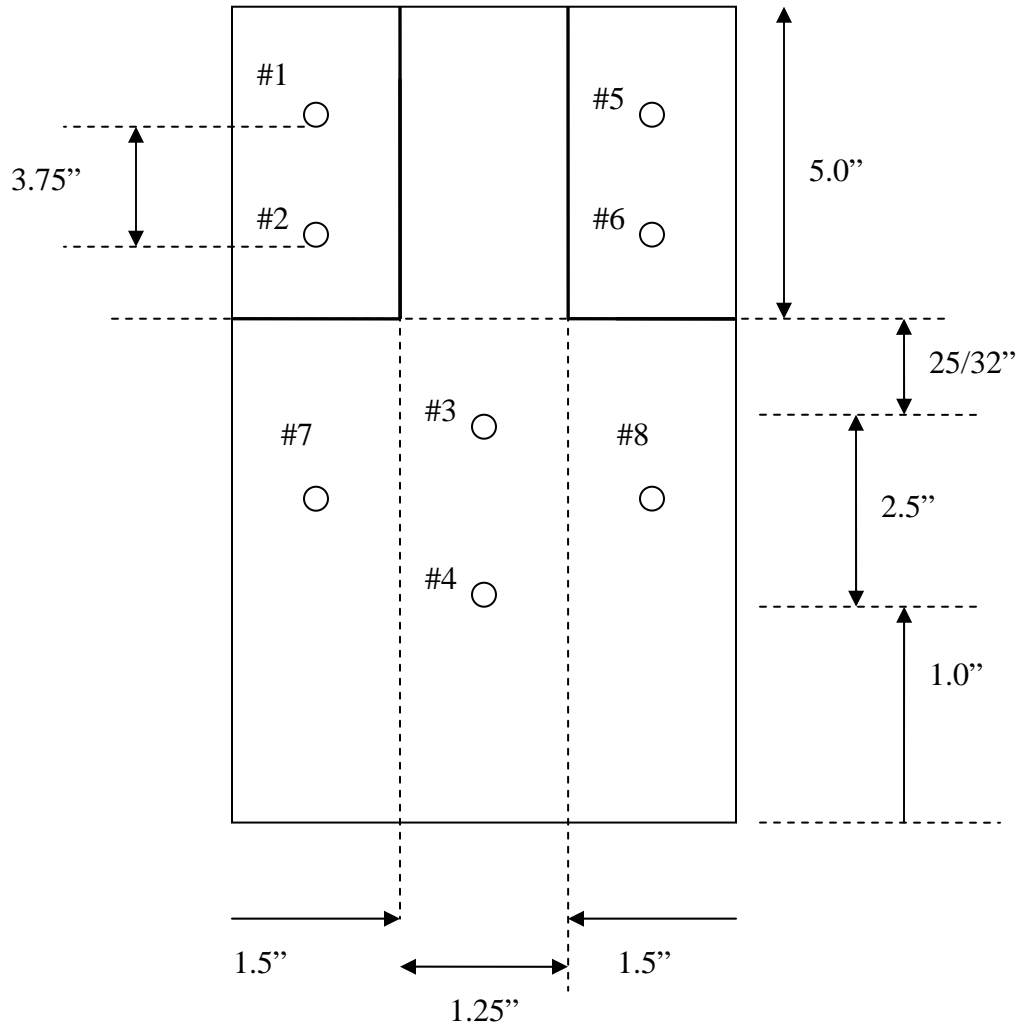


Section 5.4 Pillow Block Bearing Mounting Plate

LxWxH = 9.28x4.25x0.25"

The following piece was made to install the jackshaft mounting blocks. Holes # 7 and # 8 are used for a clamp to stabilize the plate. Before the clamp was used, the plate was offset, and the clutch assembly was mis-aligned. #3 and #4 are used to center the plate about the seat tube. They are not strong enough to keep the plate from shifting left and right. By using the brace (#7 and #8), we were able to adjust the position of the clutch about the seat tube such that the large timing belt would align with the small timing belt affixed to the motor shaft.

Holes	Screw	Drill	Type
#1, #5	5/16-18	21/64	Clearance
#2, #6	5/16-18	21/64	Clearance
#3	10-32	#21	Clearance
#4	10-32	#21	Clearance
#7	1/4"	17/64	Clearance
#8	1/4"	17/64	Clearance

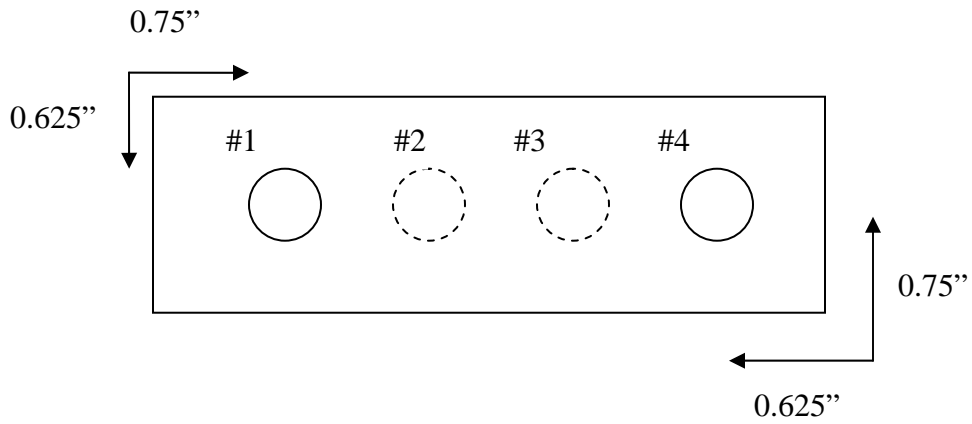


Section 5.5 Jackshaft Mounting blocks (2)

LxWxH = 5.0"x 1.5"x 0.625"

The holes with the dotted line are on the opposite side of the block. These holes are used to mount the blocks onto the plate. The holes with the solid lines are used to install the pillow block bearings. The solid bolt holes are spaced

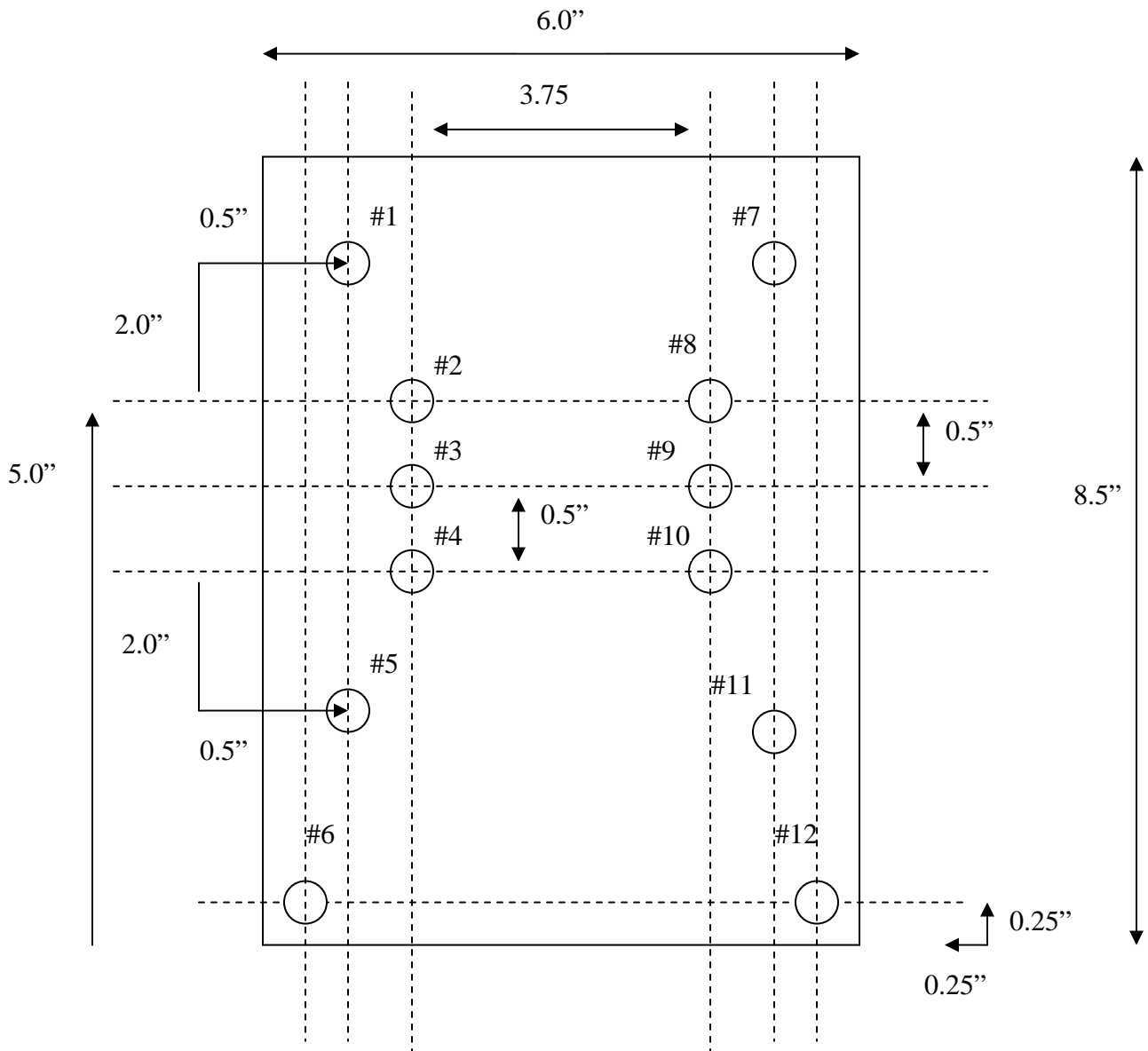
Holes	Screw	Type	Drill
#1	5/16-18	Tap	F
#2	5/16-18	Tap	F
#3	5/16-18	Tap	F
#4	5/16-18	Tap	F



### Section 5.6 Motor Mount Plate

The motor mount plate is a 1/2" thick piece of aluminum that is 6x 8.5". It is the plate that the motor cover, control box and motor are mounted to. The motor mount plate enables the motor to be placed in three orientations with respect to the clutch and timing belt assembly. The mounting locations are separated by a 1/2".

Holes	Screw	Type	Drill
#1,5,7,11	1/4"	Clearance	17/64
#2,3,4,8,9,10	mm	Clearance	1/4
#6, #12	1/4		17/64



### Section 5.7 Modifying the sprocket

The sprocket needed to be modified to avoid the chain stay. To solve this problem we asked “Smitty” to bore out the sprocket to a diameter of 2.05”, so that it could fit over the hub flange. In order to be clear of the chain stay we determined that the sprocket needed to be set 0.6” closer to the center of the hub. We had “Smitty” weld what was left of the sprocket to one end of a 2” diameter steel pipe that had been cut down to 0.6” lengthwise. On the other end of the pipe “Smitty” welded the original bolt pattern on to the steel pipe. This solution enabled us to continue using the disk brake compatible hub for our chain drive. Furthermore, we did not have to make any modifications to the wheel, which was preferable.

## **Part VI. Electrical System Design**

### 6.1 Section Overview

This section of the paper is focused on our methods for integrating the motor controller into the system for regeneration and forward drive. It is centered on the microcontroller function as the brains of the system. We look at the various inputs to it, and outputs from the motor controller which dictate the behavior of the complete system.

### 6.2 PIC Selection

We determined the PIC16F873A microcontroller, for the following reasons:

1. Past experience with programming and debugging through E72 course
2. In-Lab availability of software and programming utilities
3. Smaller than handi-board, and can be easily adapted to system
4. Two PWM output pins (CCP1 and CCP2)
5. 2 digital I/O ports ( B and C)
6. Set of analog input pins with on-board A/D converter

Our main concern with selecting a PIC was both its explicit financial costs as well as the implicit costs of having to purchase the evaluation boards and software for controlling the PIC. We also did not want to spend a lot of time learning to program another manufacturer’s PIC or adapting one of the Handiboard controllers (used to control servo motors and drive LED displays) to our system. Given the number of input/output (Digital and Analog) pins available on the PIC16F873A, we thought it would enable us to

meet our objectives of (1) motor control, (2) and feedback and safety communication between the PIC and other circuit elements.

The primary input to the PIC is the throttle input and the primary outputs are the PWM signals used to drive the motor control circuit. These inputs and output are the basis of the motor control circuit, whereas the other I/O devices are designed for optimization and safety.

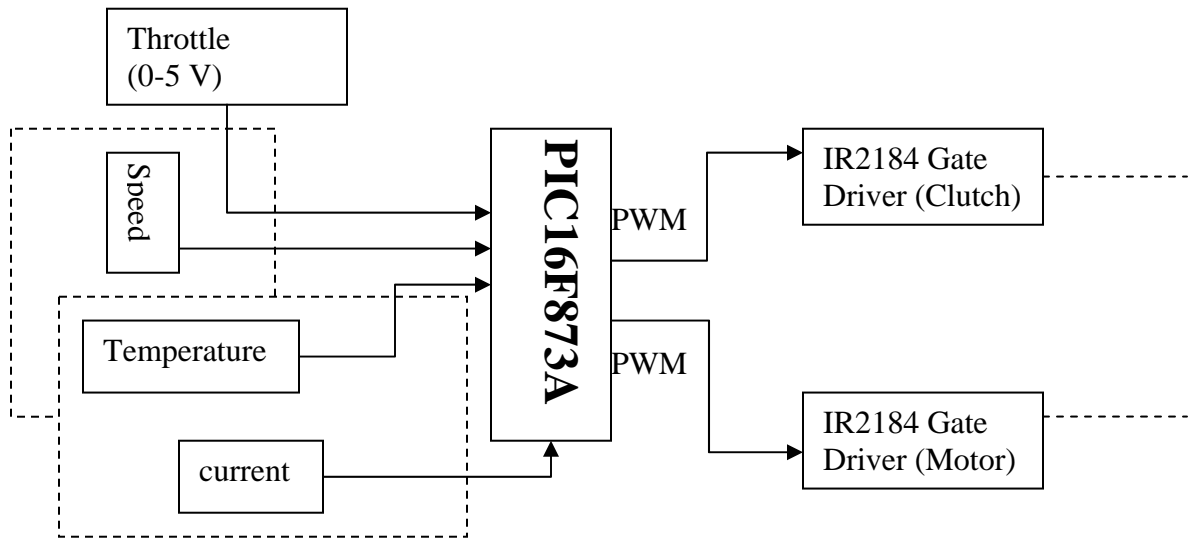


**Figure 9: Electronic Control Circuit**

Section 6.3 Throttle Input & PWM Speed Control

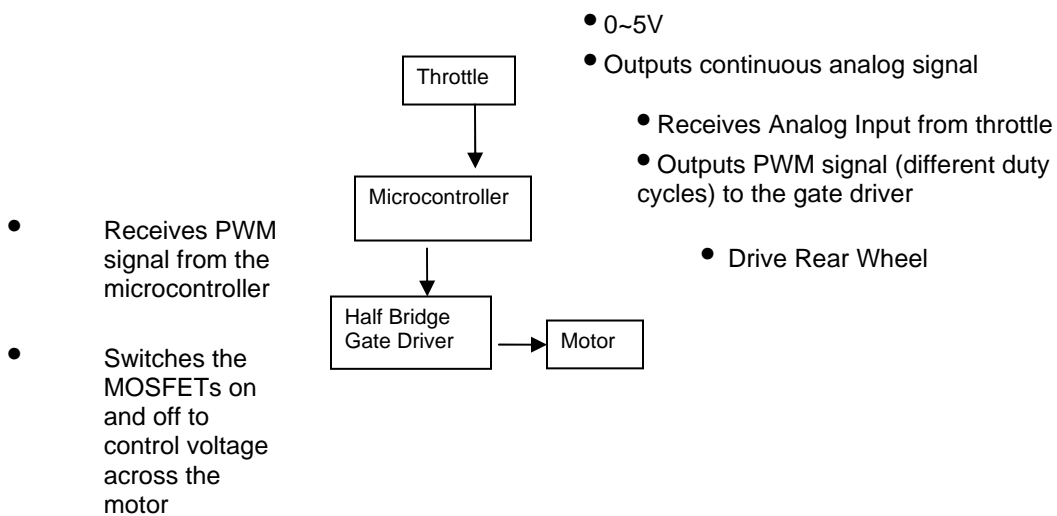


**Figure 10: Motor Control Circuit**

As shown by the figure above the throttle is a device that is connected across a fixed input voltage (5 Volts) and that outputs a variable voltage on the output pin, wiper. A lot of applications tend to use a variable resistor (potentiometer) as a throttle. These tend to dissipate a lot of heat as the current flows through the coil of wire. Since we wanted to limit the inefficiency of the system, we chose to use a Hall-Effect throttle. These do not rely on an internal resistive element to adjust the wiper voltage, but instead are based on properties of magnetism. Choosing a Hall Effect throttle increased the efficiency of the system at no extra costs.

As shown in the diagram the throttle output is then routed to one of the analog input pins of the microcontroller and is used to adjust the duty cycle of the PWM signal used to drive the motor and clutch control circuits.

The basis of our control method is pulse width modulated speed control. Under PWM, we can control both the forward drive and regenerative functions of the motor control circuit through manipulation of the PWM signal's duty cycle. We chose to use PWM control because it is easy to implement, and can conserve power if implemented at the right frequencies. Rather than using a potentiometer, which dissipates a lot of heat to control the voltage across the motor, we could use a set of transistors that we switch on and off at a given frequency. If the switching frequency is high enough, the mosfets will not dissipate a lot of heat as they switch on and off. Furthermore, by using a high frequency the motor will not be noisy because the transitions from on-to-off states are much shorter than the motor can respond to mechanically. The voltage across the motor is a function of the pulse width. The DC voltage output of a PWM signal is represented by the following relationship.

**Equation 12**

$$V_{DC} = \frac{t_{on}}{t_{on} + t_{off}} V_{High}$$

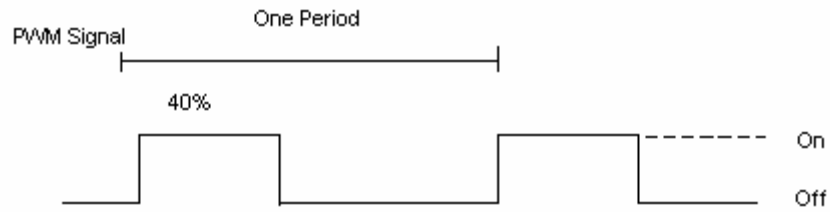


**Figure 11: PWM Signal**

For example, a 40% duty cycle yields a DC voltage that is 40% of the high pulse. Since the speed of a permanent magnet motor is proportional to the voltage across the motor, PWM control is an effective way of controlling variable speed drives like our hybrid electric bike system.

## **Part VII. Circuit Design and Implementation**

### 7.1 Section Overview

With an understanding of the basic motor controlling theory, the design and implementation of the controller is described in this part. Section 3.2 introduces the use of half bridge gate drivers and various components that are used in accomplishing speed control and regenerative braking. Section 3.3 describes the components that are used to ensure the circuit is. Section 3.4 introduces some of the feedback features that are designed to enhance monitoring and controlling of the bike. Section 3.5 puts various components together. Section 3.6 talks about the making of PCB in multisim and ultiboard.

### 7.2 Main Controller

Without going into too much detail about the design of mosfets, it is important to note their use in our design and our process for selecting mosfets. Earlier we discussed mosfets use as switches in control circuitry. We also discussed some of the benefits of mosfets including low on resistance and low power consumption when turned on. Mosfets generate the most heat during transitions from on-off or vice versa. This is because the mosfet internal resistance increases during these transitions. As a result we wanted to minimize the duration of the transitions between on and off states. Accomplishing this goal meant selecting a mosfet with a small gate capacitance such that the time constant for turning it on was fairly low. Due to the regeneration requirement, the mosfets needed to allow current to flow in either direction from source to drain or drain to source.

Because of the scale of the system, we needed to select a mosfet which could handle the amount of power being drained. Moreover they needed to be designed to operate at the voltages of the power supply and other high power devices. After looking at various mosfets available, we determined that IR3709 HEX Power Mosfets would meet the needs of our system. These mosfets manufactured by International Rectifier, are designed to operate in a 30V system and can drain as much as 90 Amps. Given our power supply is 24 V and the motor stall current is 80 Amps, one of these mosfets would be sufficient to drive the motor. IR3709 transistors have very low on resistance relative to other high power mosfets, and as a result the time constant,  $\tau = RC$ , is fairly low. Power mosfets are designed with a diode that conducts from the source to the drain for reverse currents, so these mosfets were compatible with our goals of regenerating electric power.

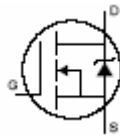


**Figure 12: IR3709 Hex Power Mosfet**

Once the mosfets were selected, we determined how they would be implemented in the system, and how we would source the current required to turn them on. To meet the basic requirements of forward drive and regeneration we only needed a half bridge circuit. This circuit arrangement is typical in applications where the vehicle is only designed for forward motion.

The current output from the microcontroller is limited and is not high enough to overcome the gate capacitance of the mosfets we chose to use. As a result we developed criteria for selecting gate drivers which would sense the PWM control signal from the microcontroller, and amplify the current on its output pins.

1. High Current Hi and Lo-side drivers
2. Minimize high and low transitions
3. Prevent Hi and Lo outputs from turning on at same time
4. Analog Input Pin for PWM signal
5. Operate on  $\geq 24$  Volts
6. Operate at 20 KHz

### Section 7.3 Gate Driver Selection

Based on the set of criteria we outlined above, we chose the IR2184 half bridge driver shown below [2]. It has digital input pins to receive the 20 KHz PWM signal coming from the microcontroller. It is designed for systems up to 600 V, and can deliver fairly high currents to turn on several mosfets at a high switching rate. We also considered the manufacturer before selecting the gate driver. Since we bought the mosfets from International Rectifier, technical representatives at International Rectifier would be able to help us troubleshoot the system more effectively.

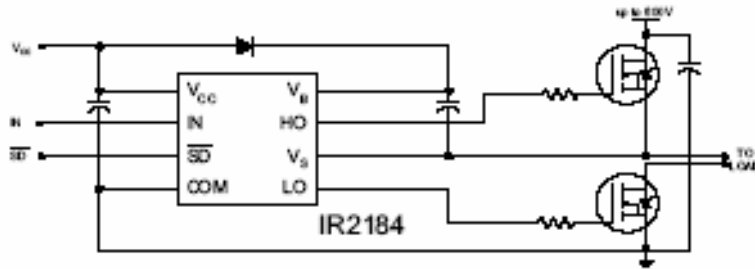


Figure 13: Typical Application <<http://www.irf.com/product-info/datasheets/data/ir2184.pdf>>

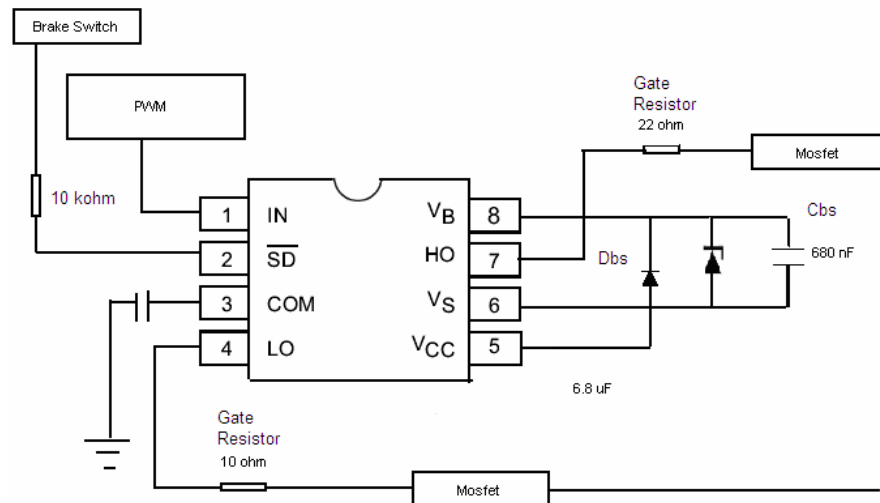


Figure 14: IR2184 Gate Driver Implementation

The above figures depict the half bridge gate driver we used to drive the mosfets. The timing diagram and table below illustrate the gate driver's functions.

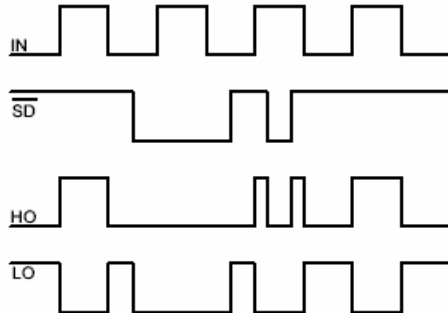


Figure 1. Input/Output Timing Diagram

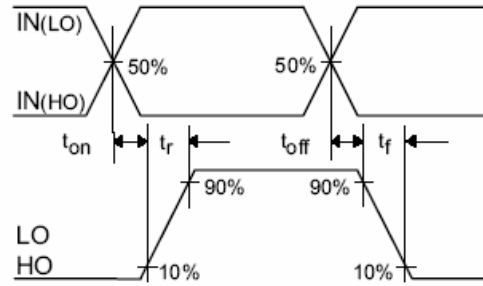


Figure 2. Switching Time Waveform Definitions

Figure 15: Input/Output Timing and Switching Waveforms <<http://www.irf.com/product-info/datasheets/data/ir2184.pdf>>

The input section of the gate driver consists of VCC, ground, IN, and SD. The following table gives a description of the function of each of the pins.

Table 6:IR2184 pin out and function

Gate Driver Pin	Name	Function
1	IN	Receives PWM signal from Microcontroller (0- 5 Volts)
2	$\overline{SD}$	Enable Pin. Normally latched to 5.2 Volts by an internal Zener clamping diode. When pulled low disables (pulls down to 0 Volts) gate driver outputs.
3	COM	Ground. Connected to VCC through decoupling capacitor.
4	LO	Switching output that is out of phase with IN to control the lo-side mosfet
5	VB	Floating supply voltage connected to VCC through high speed switching diode. Used to turn on Hi-side mosfet.
6	HO	Switching output that is in-phase with IN to control the hi-side mosfet. Varies between VB and VB+VS, except in under-voltage lockout state.
7	VS	Senses voltage at negative terminal of load (Motor). Used as a reference in bootstrapping circuit for controlling voltage at HO. Ensures that VGS > V threshold when Hi-side mosfet is suppose to turn on.
8	VCC	Positive supply voltage. Powered directly from System Batteries.

Some additional features of the gate driver include under-voltage lockout. This is important because it keeps the mosfets from turning on when the supply voltage is lower than a threshold. Another feature is a pre-programmed dead-time to control the transition time of the high and low side mosfets. The gate driver prevents both outputs from ever being high at the same time. This prevents shorting the motor

and is one of the main benefits of using a gate driver to control the half-bridge. In the next section, we will describe the half-bridge circuit and then go into some of the difficulties we encountered when trying to test our specific gate driver.

Two IR2184 Half-Bridge Gate Drivers were used in the final circuit. One was used for motor controlling while the other one was used to engage/disengage the clutch as shown below. The major difference between the clutch circuit and the motor is that we did not need to use the HO pin for controlling the clutch. Another difference is that the PWM signal is fixed at 50 duty cycle since we don't need speed control for the clutch. The main reason for using the gate driver in the clutch control circuit was to coordinate the clutch and motor circuitry. As shown in the diagram, the brake both disables the clutch driver circuit as well as the motor driver circuit. This design complemented our goal of system integration and centralizing the control of the system via the microcontroller.

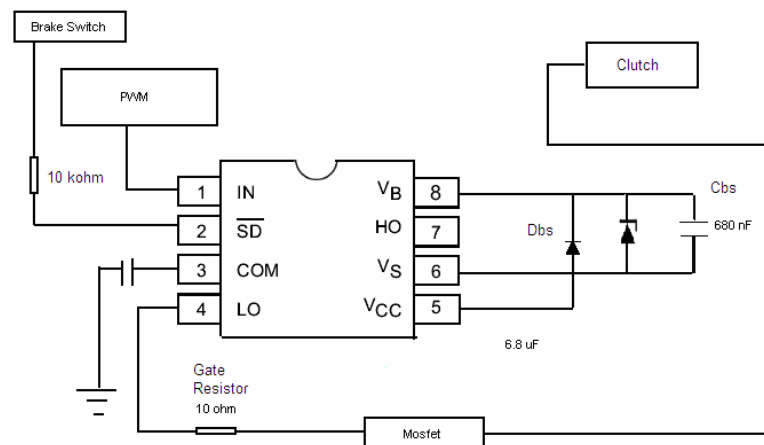


**Figure 16: Gate Driver circuit used to control the clutch**

Section 7.4 Half-Bridge Circuit Function

The motor control section of our controller is represented by the Half-Bridge driver circuit shown in the following diagram.

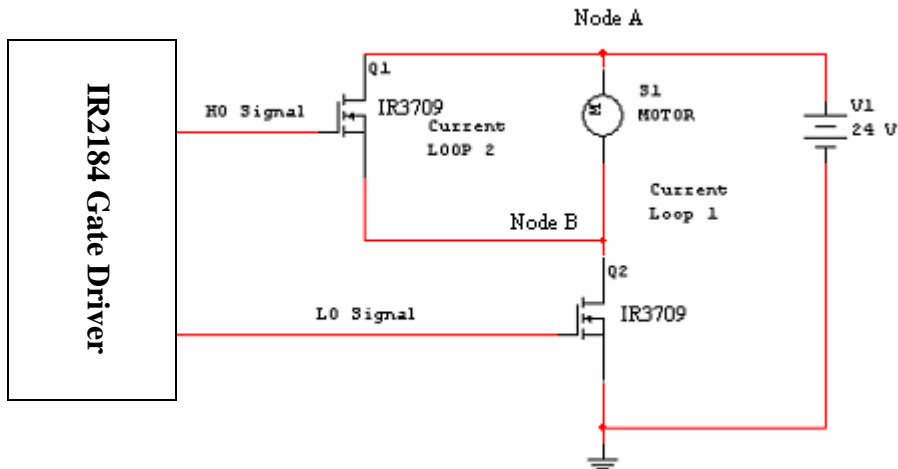


**Figure 17: Motor Control through half-bridge circuit**

Before presenting an analysis of the circuit, a few guidelines were required relating to the motor and the function of the mosfets in the circuit.

- 1) A permanent magnet dc motor can be represented by an inductance, resistance, and back-emf (voltage source) as shown in the diagram below.

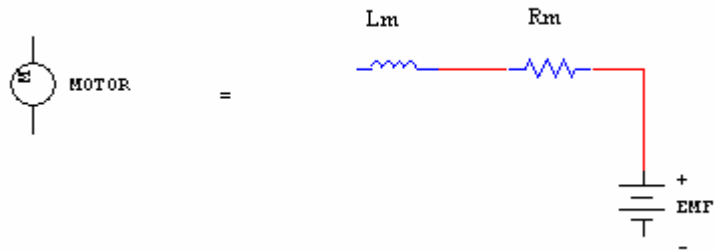


**Figure 18: Motor Simplification**

- 2) The mosfets function as switches. Given a high pulse the switch turns on. When the input is low, the switch turns off.
- 3) The gate driver's internal circuitry prevents both mosfets from ever being on at the same time. As a result current can only flow through loops 1 and 2, but never through loop 3 which result in shorting the motor. This is a safety feature integrated into the gate driver (IR2184).
- 4) Given both transistors can never be on at once, the gate driver outputs HO and LO are 180° out of phase. As a result Q1 is on (1-D) % of the time and Q2 is on D% of the time.

- 5) Current flows bi-directionally through the transistors facing negligible impedance except the motor's  $R_m$ .

Given these constraints, we have included a table below describing the modes of operation given the state of the transistors Q1 and Q2.

**Table 7: Circuit States and functions**

State	Q1	Q2	Loop	Circuit Function
1	On	Off	Loop 2	During this condition the battery is disconnected from the circuit. The loop is used for circuit protection. When the motor is switched off, a large current is developed due its internal inductance. <sup>8</sup> By having the top mosfet in the circuit there is a path for the current to be dissipated through the circuit.
2	Off	On	Loop 1	Forward drive or Regeneration depending on the duty cycle. Current flows counter clock-wise during forward drive and clockwise during electrical regeneration.
3	Off	Off	N/A	When both transistors are off, there is no path for current to flow. This is the off state for the motor.

The state of the circuit we are concerned with is state 2. Given the information that we have already outlined the following equations can be used to analyze the regenerative as well as forward drive functions of the circuit. The goal of these equations is to illustrate the dependence of the battery current on the duty cycle which the rider can control via the microcontroller.

By inspection, the voltage at node A is the same as the battery voltage.

**Equation 13**

$$V_A = V_{BATT}$$

Given the mosfets negligible on resistance (3 mOhms) and the fact that Q1 conducts only (1-D) % of the time, the voltage at node B can be estimated by

**Equation 14**

$$V_B = V_{Batt} \cdot (1 - D) \quad (1)$$

---

<sup>8</sup>  $P = \frac{1}{2} Li^2$ , when Q2 opens current still needs a path to flow because it cannot change instantaneously through an inductor. There is a large change in the current with respect to time which causes a voltage spike (back emf). Loop 2 is in the half bridge driver to assists in dissipating this energy during transition states.

Now that we have solved for both the voltages at node B and node A, we know what the voltage is across the motor at all times,

$$V_m = V_{A-B} = V_{Batt} - V_{BATT}(I - D) \quad (2)$$

, which simplifies to

$$V_m = V_{Batt} \cdot D \quad (3)$$

Neglecting the motor's inductance, we can also describe the voltage across the motor by the following equation.

$$V_m = V_{emf} + I_m R_m \quad (4)$$

By equating the previous two equations we can solve for the motor current, whereby

$$I_m = \frac{V_{BATT} \cdot D - V_{emf}}{R_m} \quad (5)$$

Since the battery current only flows D% of the time<sup>9</sup>, it is represented mathematically by the following equation

$$I_{Batt} = D \frac{V_{BATT} \cdot D - V_{emf}}{R_m} \quad (6)$$

Since we know that regeneration occurs when the battery current is negative we can use these mathematical relationships to determine at what duty cycles the battery current will flow negatively (regeneration) or when it will be positive (forward drive). See the table below for various characteristics of the circuit.

**Table 8: Modes of circuit operation as a function of the duty cycle**

Condition	$I_{Batt}$	Function
$D = 0$	0	No regeneration of acceleration drive
$D = \frac{V_{emf}}{V_{Batt}}$	0	No regeneration or acceleration
$D < \frac{V_{emf}}{V_{Batt}}$	< 0	Regeneration

<sup>9</sup> Q1 is only on D % of the time.

$D > \frac{V_{emf}}{V_{Batt}}$	$> 0$	Acceleration
--------------------------------	-------	--------------

Based on the equations, regeneration occurs when the duty cycle is  $> 0$ , but less than  $\frac{V_{emf}}{V_{Batt}}$ . Because the

battery current is zero when the duty is 0 and where the duty =  $\frac{V_{emf}}{V_{Batt}}$ , we can derive the maximum

regenerative current (minimum battery current) as a function of the duty cycle.

$$\frac{\partial I_{BATT}}{\partial t} = \frac{2V_{BAT}D - V_{bemf}}{R_{motor}} = 0 \quad (7)$$

$$I_{BATT(\min)} = I_{regen(\max)} @ \frac{\partial I_{BATT}}{\partial t} = 0$$

$$\text{Which occurs when } D = \frac{V_{bemf}}{2V_{BAT}} \quad (8)$$

Below is a graph based on the theory we have outlined in this section. In the next section of the paper we will present the results of circuit tests that proved the correctness of the set of equations developed so far.

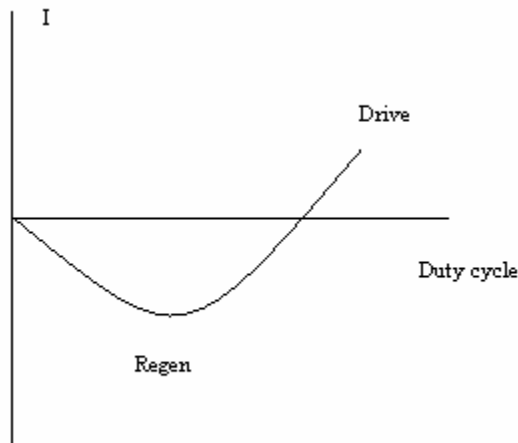


**Figure 19: Battery current as a function of the duty cycle**

### Section 7.5 Testing regeneration model & control circuit

After developing the theoretical model for our motor driver, we designed experiments to test the model's accuracy. We determined that we would test the circuit to observe electrical regeneration inside the lab, and thus at a much smaller scale than the actual system. The model we used in the lab included the following components and is shown in the diagram below.

**Table 9: System Analogs**

<b>Model Components</b>	<b>System Analogs</b>
1. 24 Volt PMDC connected via control circuit.	600 Watt, 24 Volt PMDC motor
2. Coupling shaft to connect the two motors	Power transmission system
3. Independent power supply to apply constant DC voltage across coupled motor	Rider pedaling the bike or transfer of potential energy to kinetic energy going down a hill.
4. 24 Volt PMDC motor connected across constant voltage source	Pedaling the bike.

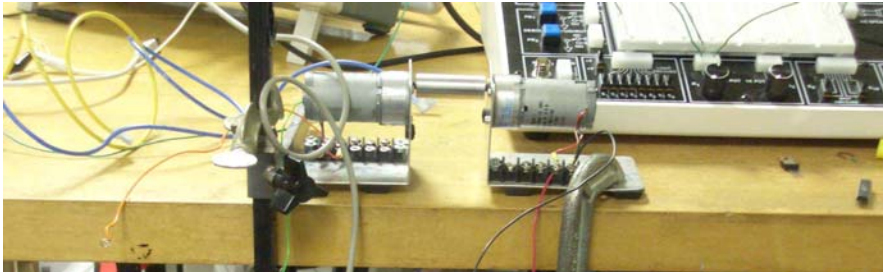


**Figure 20: Test Setup for forward drive and regeneration**

Through this setup, we were both able to observe the braking force during regeneration as well as record the battery current by inserting an ammeter into the circuit. We observed the complete duty cycle, and thus observed the transition from regenerative functions to forward drive. As stated in the table, and in an earlier section of the paper, the amount of regenerative current is proportional to the rider's effort through pedaling or the steepness of a hill which contribute to the overall speed of the mechanical system through energy conversion processes.

The motor can only generate a certain amount of speed limited by its speed constant we solved for earlier. By adjusting the voltage of the coupled motor, we modeled how the amount of current regeneration would change given an increase in the rider's effort. Below are graphs showing how the regenerative capability of the system varied as the voltage across the coupled motor changed.

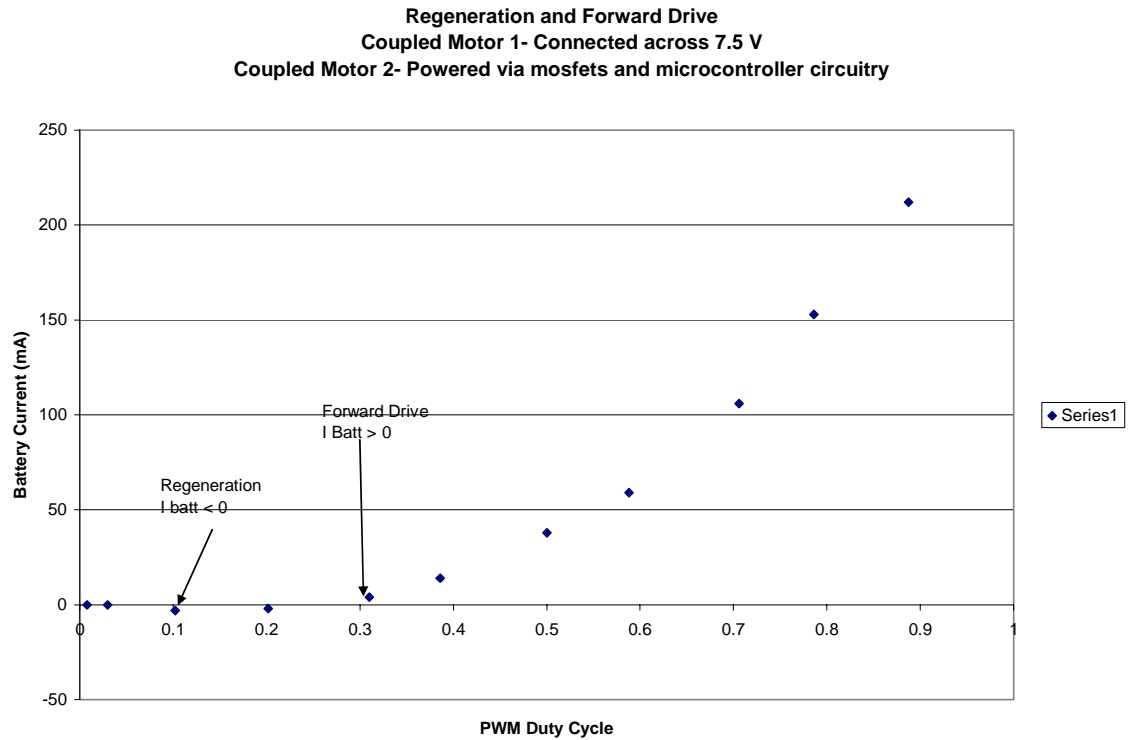


**Figure 21: Coupled Motor loaded at 7.5 Volts**

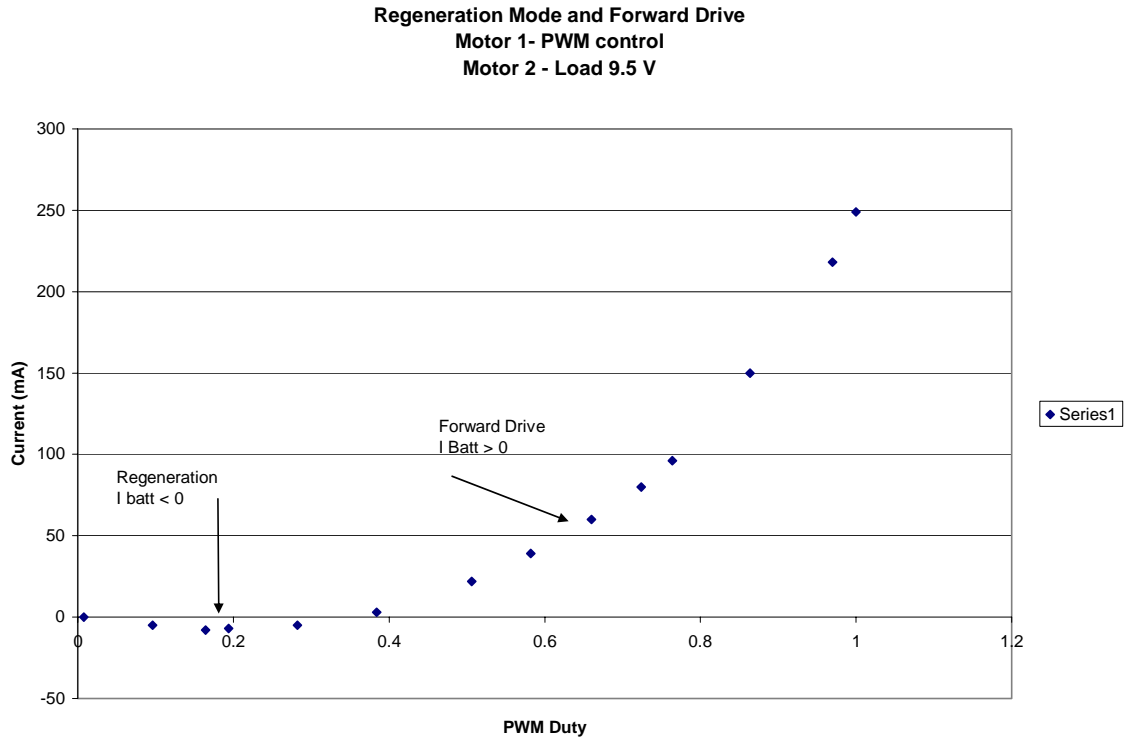


**Figure 22: Coupled motor loaded at 9.5 Volts**

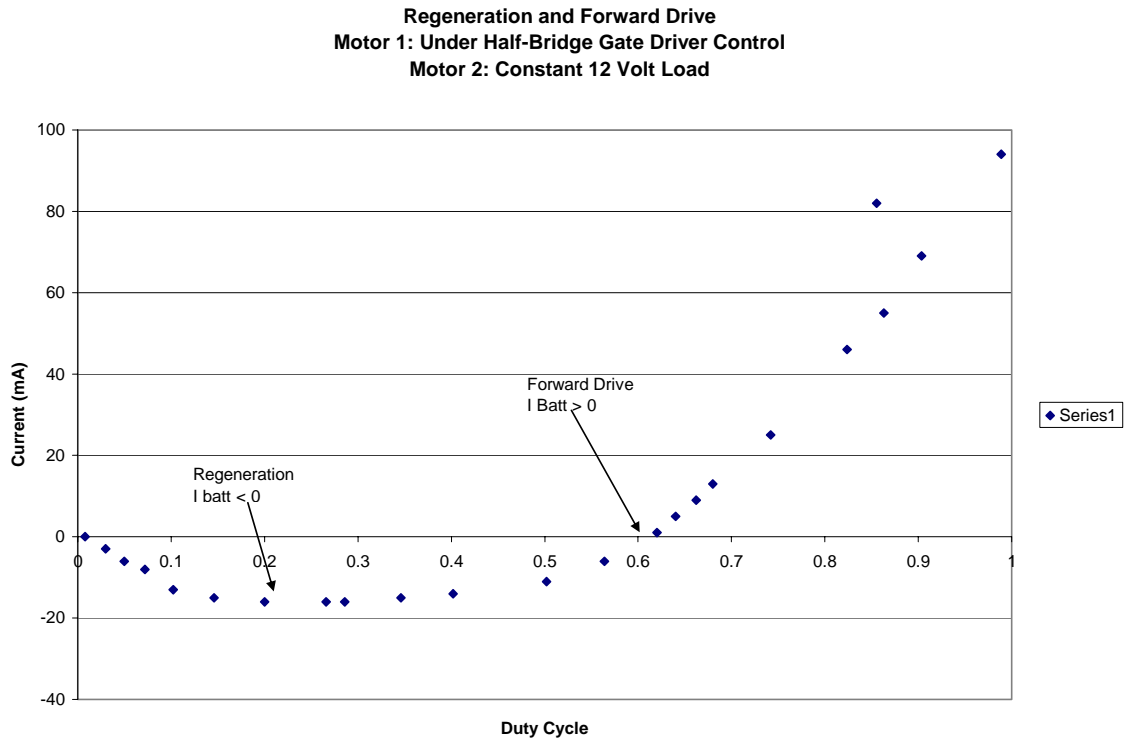


**Figure 23: Coupled motor loaded at 12 Volts**

It is evident from the graphs that as the voltage across the coupled motor increased the regenerative capacity of the system also increased, such that a larger proportion of the duty cycle was allocated to regeneration. When the coupled motor contributed less to the speed of the system, the forward drive condition dominated. These results are consistent with our earlier discussion of regeneration and various motor constants use to characterize PMDC motors performance.

#### Section 7.6 Implications of regeneration for entire system

Electrically, the effect of regeneration is fairly simple. When negative current flows through the system, the batteries are charged. By facilitating this process, we hope to extend the electrical range of the system, such that the bike can travel for longer distances without having to recharge the batteries. This makes the bike a more practical alternative to other modes of transport.

Mechanically, regeneration causes braking. Based on the relationships we saw earlier between torque and current, a negative current creates a negative torque. If the bike is in linear motion, this negative torque will create drag on the system, thus slowing it down. This is useful for speed control, but may be undesirable in certain situations where the rider wants to travel at maximum speed. Regeneration entails converting kinetic energy into electrical energy, and partially braking the system through generating reverse torques, is much more efficient than relying solely on the bikes pad (friction) brakes.

#### Section 7.7 Problems with using the IR2184

The gate driver is fairly simple functionally. However, it was more a difficult task selecting the circuit elements which complemented its functions. As shown in the circuit, selecting the correct size diodes, resistors and namely capacitors was critical for getting the gate driver to function properly. Our main difficulty was getting the HO output to function correctly. When the capacitors are not selected appropriately, the under-voltage lockout feature of the gate driver is invoked thus, disabling motor control. As we said before, the voltage at HO is a function of a bootstrapping circuit required to boost the voltage at the gate of the hi-side transistor. If the capacitor is either too small to appropriate the required charge or too large to charge within the specified time (long time constant), the device goes into the under-voltage lockout state.

The voltage at pin VB is obtained by the **bootstrap method**. [3] When the low side channel is on,  $V_S$  is pulled low, and the bootstrap capacitor  $C_{BS}$  (see above figure) discharges through the low side mosfet while the Hi-side mosfet is turned off. When the lo-side mosfet is off,  $V_S$  is the voltage at the – terminal of the motor (load), and the bootstrap capacitor charges. Through internal circuitry, we won't explain in this paper, the HO pin's voltage is allowed to vary between  $\approx V_S$  (off state) and  $V_B + V_S$  (on state). Because, the capacitors we initially selected did not meet the specifications required for this application, the gate driver stayed in an under-voltage lockout state.

In selecting the capacitor, the major challenge was selecting one with the right capacity to handle the charge, and that could charge fast enough to meet the other goals of the circuit ( $\tau \ll 20\text{kHz frequency}$ ). As a result, we contacted International Rectifier to get information on selecting the bootstrap diode and capacitor. We selected the IN914 diode as our bootstrapping diode. It was suggested by the manufacturer of the gate driver since it has a sufficient reverse breakdown voltage and current switching rate to both protect the power supply and complement the speed at which we wanted to charge the bootstrap capacitor. Finally, the bootstrap capacitor is determined from the following formula [4]

**Equation 15:**

$$C \geq \frac{2[2Q_g + \frac{I_{qbs(max)}}{f} + Q_{ls} + \frac{I_{Cbs(leak)}}{f}]}{V_{cc} - V_f - V_{LS} - V_{min}}^{10}$$

where

$$V_{cc} = 24V$$

$$V_f = \text{Forward voltage drop across the bootstrap diode}$$

$$= 0.72\text{V(max)} (\text{Philips 1N914 High Speed Diode Spec Sheet})$$

<sup>10</sup> See International Rectifier DT 98-2a <http://www.irf.com/technical-info/design/tp/dt98-2.pdf> or AN978-b at <http://www.irf.com/technical-info/appnotes/an-978.pdf>

$V_{LS}$  = Voltage drop across the low side FET

$$V_{LS} = R_{DS} I = R_{DS} Q_g f$$

$R_{DS}$  = Static Drain - to - Source On - Resistance

$$R_{DS} = 9.0 \mu\text{ohm}(\text{max})(\text{IRF3709 Spec Sheet})$$

$Q_g$  = Total Gate Charge at the transistor

$$Q_g = 41 \text{ nC} (\text{IRF3709 Spec Sheet})$$

$f$  = frequency of the duty cycle = 20 kHz

$V_{Min}$  = 10V (Minimum voltage between  $V_B$  and  $V_S$ )

$I_{qbs(\text{max})}$  = Quiescent  $V_{BS}$  supply current = 150 (microamp, max)

$Q_{ls}$  = 5nC (Level Shift Charge required / cycle) (Design Application Note AN978a)

$I_{Cbs(\text{leak})}$  = 0 (Only applies to non - electrolytic capacitor)

Based on the calculations the minimum bootstrap capacitor that could be used in this application is 257nF. Ultimately, we chose a 680 nF ceramic capacitor because of its good test results.

Another important calculation regarding the gate driver was the number of mosfets it was able to drive at the same time. That is determined by dividing the total amount of gate charge from the current that is sent out from the gate driver with the time period being the transistor turn on time.

**Equation 16:**

$$N = \frac{I t_{on}}{Q_g} \quad (1)$$

and

$$Q_g = 27 \text{ nC}(\text{typical}), 41(\text{max})$$

$$I = 1.9 \text{ amp}(\text{Given in IR2184 datasheet})$$

the turn on time of the transistor is given by

$$t_{on-\text{delay}} + t_{rise} + t_{fall} = 11 + 171 + 21 = 203 \text{ ns} \quad (2)$$

For a typical application,

$$N = \frac{I t_{on}}{Q_g} = \frac{1.9 \text{ amp} \cdot 203 \cdot \text{ns}}{27 \text{ nC}} = 14$$

We see that the gate driver is capable of driving 14 gate drivers under typical situations.

## Section 7.8 Power & Safety Circuitry

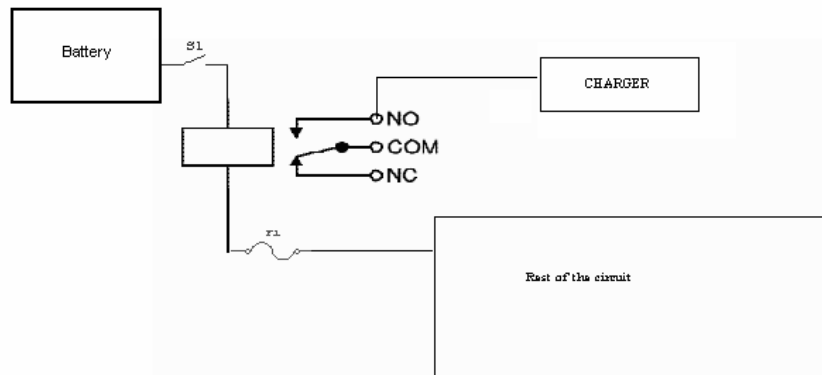


**Figure 24: Circuit Isolation Components**

The safety components designed for the circuit include an automatic shutdown switch, a 40 amp relay (electromagnetic switch) and two 35 amp fuses. The user can conveniently turn on and off the controller by toggling the automatic shutdown switch. It appears redundant that we have both a SPST switch and relay in the same circuit. However, the reason why we used both a relay as well as a low current SPST switch was due to the difficulty we encountered in finding an SPDT switch with contact ratings similar to the relay. Since, the switch is designed to break the circuit, its contact ratings would have needed to be rated as high as other high-power elements in the circuit. When the switch is closed, the 40 amp relay will be connected to the circuit and provides a path for power to flow from the battery to the rest of the circuit.

The relay functions as a SPDT switch and can either connect the battery to the charger or to the circuit. This was a convenient solution for integrating the charger into the circuit. We were concerned as to how we would isolate the charging of the batteries from the rest of the circuit, which drain current from the batteries. By using the SPDT relay we ensure that the entire charger current is transmitted directly to the batteries. We were able to make the circuit safer through giving the rider an automatic shutdown outlet, but also achieve another goal of enabling the batteries to be charged without removing them from the mounting assembly.

If the current going into the circuit exceeds 70 amps, the fuses will melt and disconnect the power source from the motor. This is perhaps overprotection since the relay, which is closer to the power source,

is only designed for 40 Amps. Given the function of the relay, and the unavailability of larger relays that were PCB mountable, we have to accept this current limit.

The microcontroller can also be used to ensure safety within the system, as it receives inputs from various sensors within the circuit. Depending on the outputs of those sensors, the microcontroller can be programmed to disable certain circuit functions.

## **Part VIII. Feedback Features & System Integration**

### Section 8.1 Overview

The motor controller would not have been complete without implementing hardware or software to sense the system state and provide outputs that could adjust the state of the system to operate within certain conditions.

### Section 8.2 Brake and toggle switch

The first of these feedback mechanisms are the various shutdown switches which includes the handlebar brakes and the toggle switch found on the control box. While the brake can bring the bike to a stop, it is only a temporary stop since the rider has to compress it for as long as he/she wants the motor to stop (clutch disengage). Because the brake switch is normally open we determined that the best place to implement it was at the enable pins of the gate driver. When the rider wants to stop the bike temporarily he simply squeezes the brake lever, thus causing the brake pads to engage the wheel but also pulling the gate drivers  $\overline{SD}$  pin low. On the other hand, the toggle switch takes electric power away from the motor controller permanently. After turning the switch to its off position the electrical system is disengaged, but the bike has to come to a stop on its own, unless the brake levers are compressed. The brakes are simple feedback units.

### Section 8.3 Speed Sensor

In addition to the relatively simple feedback units, we designed the system to sense speed and temperature, with the temperature controller being the most complicated.

The speed sensor we chose to implement was fairly cheap and easy to implement. The only hardware was purchasing a magnetically actuated switch which could be mounted to the front fork of the bike frame, and a magnet (actuator) that would be mounted to the wheel. The major consideration affecting

our selection of a magnetic switch was its sensitivity. Fortunately, we were able to find switches made by Amseco which had a range of 2”.

The switch is a normal Single pole single throw switch with one connection to ground and another connection to 5 V through a pull up resistor on the PCB board. During each revolution of the wheel the actuating magnet aligns with the reed switch and causes its contacts to either close or open depending on whether the switch is normally open/closed (NO or NC). As the switch opens it sends a voltage pulse of 5 volts to one of the digital I/O pins of the microcontroller. Using the microcontroller’s on-board clock the period of the pulses was determined. After processing, we most likely would compare this with the desired speed given the throttle input, and implement a control strategy (PID) that would safely allow the electro-mechanical system to adjust its performance to match the rider’s expectations for speed.

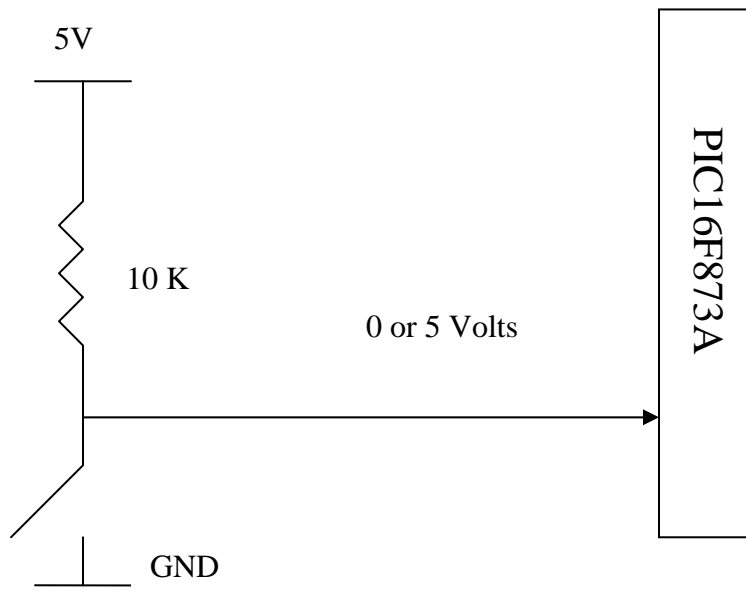


**Figure 25: Speed Sensing Circuit**

Some of the considerations we took into account when purchasing the switch was its susceptibility to noise or premature activation due to bumps. Depending on the orientation of the switch on the fork, it will be more or less likely to close or open when there is a sudden shock. If the switches are placed vertically, we should alleviate this problem.

We chose reed switches for their simplicity and durability. We did not have to worry about protecting them as much as we would have had we used optical sensors.

Currently, the pulse detection software for the tachometer is complete, but the control software has not yet been written for the tachometer assembly.

#### Section 8.4 Temperature sensor

One of the major concerns for the circuit components is preventing overheating. Since the control box, motor and other electrical components are not isolated from the rider, it is important that the temperature of these devices does not exceed certain thresholds. The operating temperature of most of the devices on board is between -40 and 150 degrees Celsius. Obviously, this range is not acceptable for humans, but given that the system would be too constrained if forced to stay within a very narrow temperature range, we were primarily interested in the performance ratings of the devices. After all, the motor, microcontroller, batteries, transistors, etc. can only operate predictably within certain ranges, whereas a human can know not to touch components on the PCB after they have been on for long durations.

Before selecting the temperature sensor, we were faced with the following constraints.

1. Operate outside the largest range of temperatures for the existing circuit components
2. Have a low costs
3. Facilitate system control via communication with the microcontroller
4. Capable of bypass the microcontroller to directly control the system
5. Minimal amount of interfacing hardware (wires,

Based on the set of criteria we selected the TMPO1 temperature sensor from analog devices. We did not have to purchase the sensor given the small quantity we requested, and its being available as a sample. The only hardware required was the sensor itself as it senses temperature without thermocouple wires, etc. The sensor has three outputs: (1) VPTAT – an analog voltage proportional to the temperature (2) under temperature open collector output and (3) over temperature open collector output.

Below is a diagram of the TMPO1 temperature sensor.

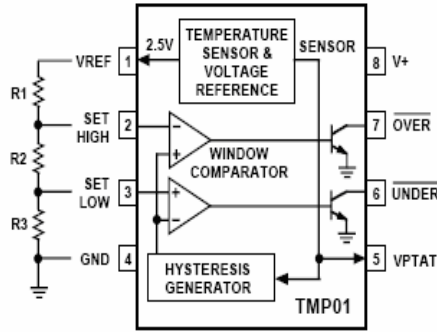


**Figure 26: TMPO1 Temperature Controller**  
[http://www.analog.com/UploadedFiles/Data\\_Sheets/21709895tmp01.pdf](http://www.analog.com/UploadedFiles/Data_Sheets/21709895tmp01.pdf)

As shown in the diagram the temperature sensor basically uses two window comparators to compare the temperature determined through a resistor ladder to a high temperature in the case of the top comparator or to a low temperature in the case of the bottom comparator. The resistor ladder is essentially a set of voltage dividers enabling the programmer to set the reference voltage for each of the comparators. The range between the over temperature condition and the under temperature condition is also determined by the values of the resistors used. The equations for setting the temperature through the resistor ladder can be found in the data sheet<sup>11</sup>.

Because we don't expect to ever have an under temperature condition, we simply tied the outputs of the  $\overline{OVER}$  and  $\overline{UNDER}$  pins of the temperature controller. When the top comparator senses a higher temperature than the Set High temperature, it turns on a transistor on its output. Until the over temperature condition ceases to be true the transistor remains on, thus providing a path to ground. One of the goals of the temperature sensor was direct control of the electro-mechanical system. We accomplished this by connected the  $\overline{OVER}$  (source of transistor) pin of the TMPO1 to both the clutch and motor gate driver  $\overline{SD}$  pins through a pull up resistor. As a result, when the temperature is within  $V_{Set\ High}$  and  $V_{Set\ Low}$ , the gate driver receives a normal PWM signal. However, whenever the temperature sensor reaches the threshold, the gate drivers are disabled.

<sup>11</sup> [http://www.analog.com/UploadedFiles/Data\\_Sheets/21709895tmp01.pdf](http://www.analog.com/UploadedFiles/Data_Sheets/21709895tmp01.pdf)

The temperature sensor's importance to the circuit is fairly high. We did not include a lot of heat sinking material on the PCB and as a result, temperature control may be an issue. Using the temperature feedback from the temperature sensor, we can ensure that our electronic devices do not sustain permanent damage due to overheating.

Using VPTAT (TMPO1 output, pin 5) we sent a continuous voltage proportional to the Kelvin temperature to the microcontroller. After A/D conversion the microcontroller could perform whatever processing or control scheme we programmed it for. Again, the variable we would control would be the duty cycle. For example, if the motor and motor controller is overheating, we would adjust the speed of the motor to one that produces less heating.

### Section 8.5 Current Sensor

Like the speed sensor, the output of a current sensor can be used in common closed loop control algorithms. Specifically, torque is a function of the current. By measuring the current through the motor, we can determine fairly accurately how much torque the motor is transmitting to the transmission system. Like all the other parts of the system we had a set of criteria for the current sensor.

1. Limit additional resistance in the circuit created by the sensor
2. Bidirectional to sense both regenerative current as well as positive current
3. Compatibility with system scale
4. Limited power consumption

We were able to find a Hall Effect Current sensor which operated off a 12 Volt supply drawing negligible current. By selecting a Hall Effect sensor we did not have to worry about resistive heat losses. The sensor itself was easily adaptable to the system as it only has 5 pins and is directly mountable to the PCB. The current sensor has one analog output, 0.1125V/Amp,<sup>12</sup>volts that could be sent directly to the microcontroller's A/D converter (port A). After A/D conversion, the torque can be calculated using the torque constant we discussed earlier in the paper. Again, the mode of adjusting the torque is by way of changing the duty cycle.

---

<sup>12</sup> Constant =  $\frac{4.5V - 0.0V}{20Amps - (-20Amps)} = 0.1125V / Amp$

Because the sensor is bidirectional, we can also observe when the circuit is regenerating current and thus, producing a reverse torque. Again, by adjusting the duty cycle we can control the amount of regeneration that occurs.

It is clear that the sensors we have chosen have both safety features as well as features that will enhance the performance of the system. We have completed the design of the system and determined how each of our sensors would be implemented in hardware. The major challenge remaining for the project lies in the software implementation of the sensors. Until the sensors are fully integrated into the system, the system will not be optimized, but will be functional.

#### Section 8.6 Other Feedback components

An additional component that we did not discuss is the accelerometer. Due to the limits of time and budget we did not explore the potential of the accelerometer for the circuit, namely in the feedback section. However, given we know a manufacturer of accelerometers and have selected an accelerometer that is compatible with the scale of our system we designed the PCB to accommodate the addition of an accelerometer. Due to limited time however, we did not purchase the evaluation board knowing we would not be able to test within the project deadline.

### **Part IX: PCB Design and Implementation in Multisim and Ultiboard**

#### Section 9.1 Electric design criteria

During the design of our circuit we used Multisim 7.0, a printed circuit board (PCB) layout and design tool that includes a graphical user interface (GUI) and various simulation interfaces. Multisim has extensive libraries of circuit components. These components are included in the GUI as virtual components. Although, many of the components are already included in component libraries, it was essential that we created the exact number of pins on any virtual components that we added. Moreover, the pin locations and sizes had to match the actual components. This process is known as creating a footprint. The footprints we created in Multisim 7 would later have to match those used in Ultiboard<sup>13</sup>, specifically those footprints we added. We later found that it was better to create the footprints in Ultiboard and assign them to a library which could then be accessed by Multisim. Because Multisim 7 and Ultiboard are both made by Electronic

---

<sup>13</sup> Graphical design software that produces actual PCB layouts and specifications that can be forwarded to PCB manufacturers who fabricate the PCB.

Workbench, they share the same component libraries when installed. See the appendix for the complete circuits represented in Multisim.

After the virtual circuit was completed in Multisim we transferred it directly to a file in Ultiboard 7.0. During the transfer of components from Multisim to Ultiboard, a series of reports describe which components were transferred and any problems that occurred during the transfer. If one of the components' footprints is not already in Ultiboard's library, it will appear as an X in Ultiboard and warning messages will appear. By first creating the component footprints in Ultiboard, we were able to minimize the occurrence of this problem. After a successful transfer, all the real components are visible within the Ultiboard design file. However, we had to arrange the components ourselves.

The arrangement of components in Ultiboard was a time intensive process. Often times, there does not seem to be a best arrangement and different compromises have to be made throughout the design process. However, as a rule of thumb, placing the components in a way that closely follows the way they were placed in Multisim is desirable as it is easy to identify components and perform troubleshooting. An additional rule is to make the connections as short and straight as possible. When copper traces are really long and distributed, there are more opportunities for shorts, faulty connections and other circuit problems. By designing the board so that the traces are as short as possible, we conserve space and minimize the overall resistance of the board, thus, conserving power. We tried our best to place the circuit elements used to make external connections on the perimeter of the board. By following this method, it was easier to connect external wires and components to the PCB.

One of the more troublesome design problems was selecting the trace widths to use for the various current loops. The traces on the PCB are usually made of copper with a specified thickness. For high current circuits, it is helpful to use heavier copper. We used the following formulas to calculate the trace width and copper areas [5]

### Equation 17

$$\text{Copper Area(mils}^2) = \left( \frac{I}{k \cdot \Delta T^b} \right)^{\frac{1}{c}}$$

$I$  (Amp) = current going through the trace

$k = 0.0647$  (external layer)

$b = 0.4281$  (external layer)

$c = 0.6732$  (external layer)

$\Delta T$  ( $^{\circ}$  C) = Expect temperature rise

1 mil =  $10^{-3}$  inch

$$\text{Width(mils)} = \left( \frac{A}{d \cdot 1.378} \right) \quad (3.7.2)$$

$A$  (mils<sup>2</sup>) = Copper Area

$d$  = Thickness of the copper (mils / oz)

We ultimately used a trace width calculator to calculate the trace widths and trace areas<sup>14</sup>.

Using a maximum current rating of 70 amp, 1.5 oz/ft<sup>2</sup> of copper, and designing for 20 degrees of expected temperature rise, we calculated a minimum trace width of 2314.4 mils (2.3"). 2.3" is prohibitively wide. Had we designed the board with traces that wide, we would not have met our goal of designing a PCB that fit the scale of our system. As a result, we developed ways to avoid designing the board with such large traces.

There are a limited set of locations on the circuit where trace widths are a problem. High currents are limited to the current loop we used to drive the motor. Within this loop, the trace coming from the relay contacts, the traces that connect the two 35 amp fuses, and the trace connecting the - terminal of the motor to the Lo-side mosfets to ground are affected. Moreover, the ground strip needed to be wide enough to drain all the current.

---

<sup>14</sup> Visit the following website for trace width calculations and equations.  
<<http://www.geocities.com/CapeCanaveral/Lab/9643/TraceWidth.htm>>

To limit the size of the traces from motor (-) through the low side mosfet we decided to use 6 transistors (IR3709) in parallel to distribute the current evenly through 6 traces. That reduces the required trace width to 158 mils. Since the relay is only able to take up to 40 amps, we used an even smaller sized trace in the actual layout.

We still needed to find a way to implement our fuses and relay connections however. Even after limiting the current to 40 amps, the trace widths were still over an inch wide. Seeing no easy way around that, we decided to make those connections as short and wide as possible without interfering with other components in the circuit. In the final circuit design, we placed additional copper (500 mils wide) on top of the traces connecting the fuses and also at the relay contacts. This was a compromise we had to make given the limited time we had to create other designs.

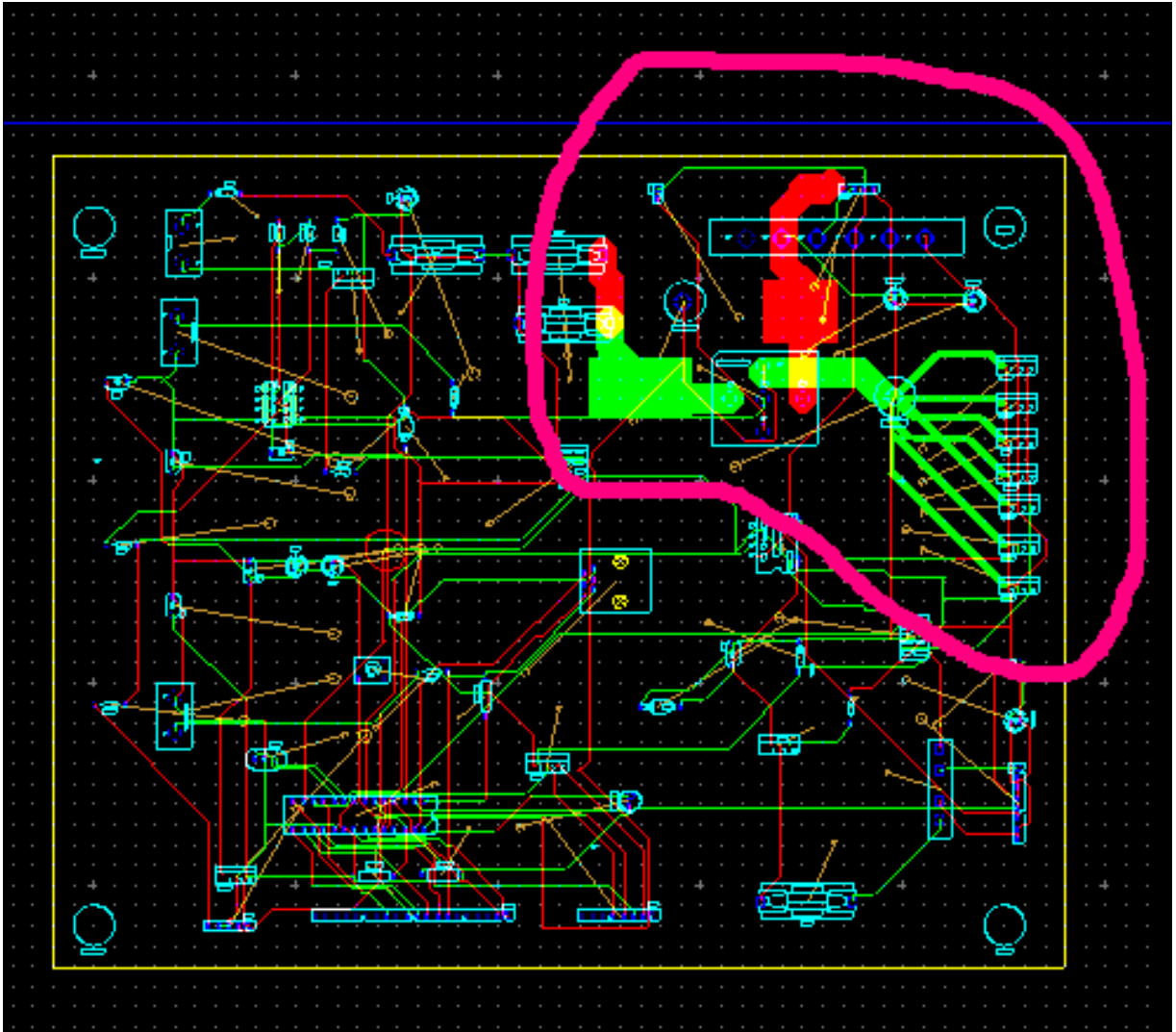


**Figure 27: Final PCB Layout in Ultiboard**

As shown in the figure above, the circled area has thick traces with additional copper placed on top of them. We specified the other trace widths by selecting their individual net-lists in Ultiboard, and applying standard design rules to the entire net-list.

One of the last problems we confronted was how to ground the circuit. Although, the entire circuit is powered from the same supply we determined that we would use one ground for the high power circuit and another ground for the low power portion of the circuit. The termination for the high-current ground is located on an isolated part of the bike. The other circuit elements utilize the second ground which is terminated at the control box.

Before completing our design, we needed to determine the radii of the drill holes used for the various connectors we wanted to add to the circuit. A number of the holes were for standard connectors, while others were simply designed as clearance for standard gauge wire. By applying the equations in this section, we could easily find the radii of the drill holes and also the pad diameters required for the various components of our circuit. For example, to calculate the diameter of the pad for a pin that can handle 70 amps of current, we used the following set of equations.

*Area of the Trace*

$$Area = \left[ \frac{I}{(k \cdot \Delta T^b)} \right]^{\frac{1}{c}} = 4783 \text{ mils}^2$$

$$I = 70 \text{ amp}, k = .0647, b = 0.4281, c = 0.7349$$

*Diameter of the pad (no.8 wire) : 128.5 mils*

*Raidus of pad + annular ring*

$$L = \pi \left( r - \left( \frac{128.5}{2} \right) \right)^2 = 4783 \text{ mils}^2$$

$$L = 150.34 \text{ mils}$$

$$R_{AR} = L - \frac{128.5}{2} = 86.09 \text{ mils}$$

After we had completed the layout, we used Ultiboard's auto-router to establish all the connections and perform error checking. When two connections were too close, the auto router draws a red circle marking the problem area. The ultiboard auto router will not finalize the circuit until all of the problems have been corrected. After completing this process, the final board outline was 8x 10". See appendix for complete Ultiboard Circuit.

### Section 9.2 Circuit fabrication

In order to conform the PCB to the system's scale, we determined that we needed to use a heavier copper, 1.5 oz/ft<sup>2</sup>~2 oz/ft.<sup>2</sup> After comparing different PCB manufacturers who used heavier copper traces, we chose APCircuits to produce our PCB due to their fast turn around and competitive prices. We designed the board in Ultiboard on two layers of copper to conserve space and allow for heat dissipation. After laying out our circuit in Ultiboard, we submitted the Gerber files (top copper layer, bottom copper layer, board outline) and NC drill file (contains drilling information) to APCircuits for fabrication. See Appendix E for pictures of our final PCB.

**Part X. System Integration & Conclusion**

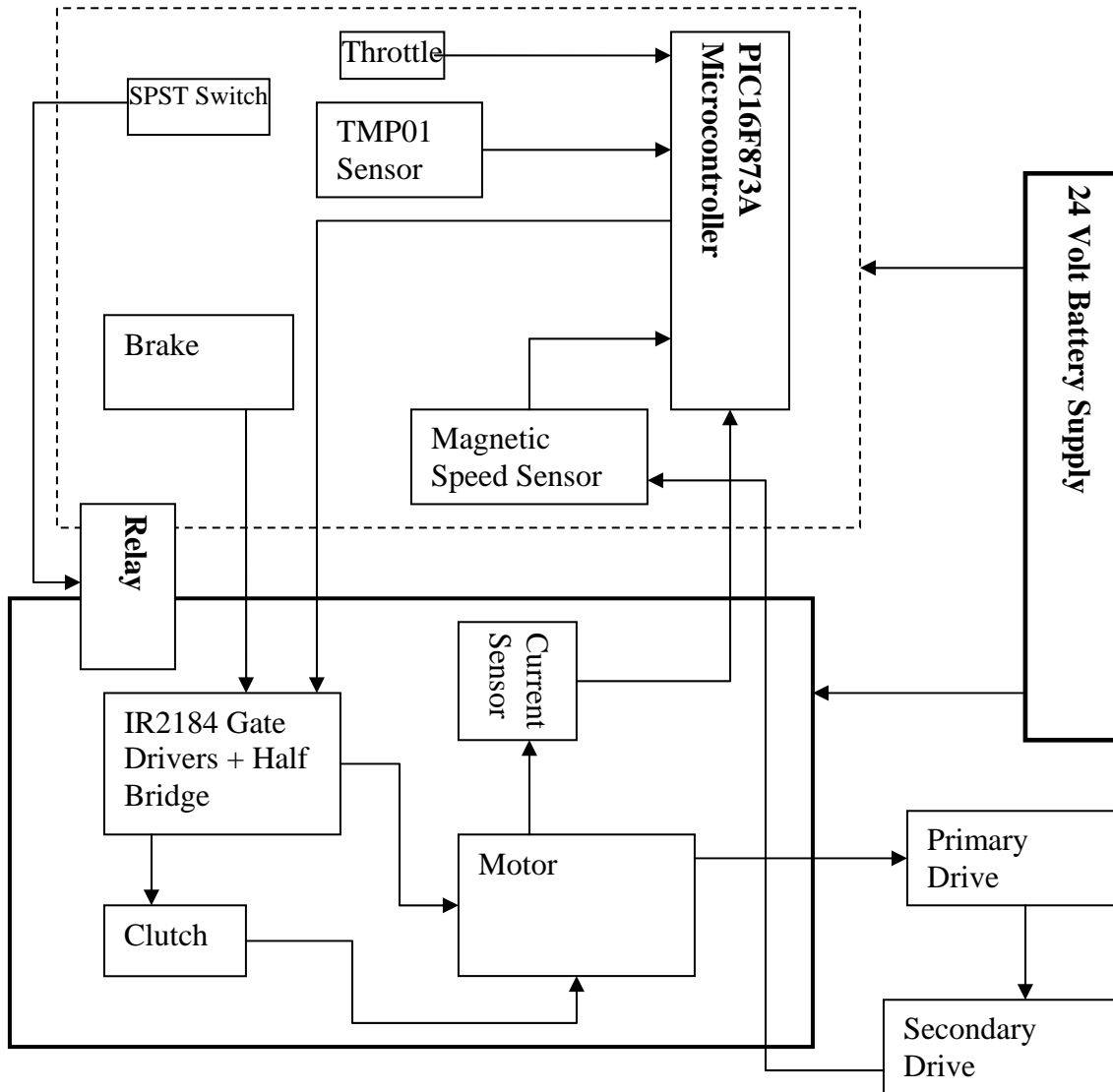


**Figure 28: Complete Circuit Layout<sup>15</sup>**

The figure above is a block diagram of the overall control system. When the automatic shutdown switch is closed, the relay will activate the circuit by permitting power into the circuit. By turning the throttle, a continuous of voltages from 0 -5 V is sent to the microcontroller's A/D conversion inputs pins. After interpretation of the throttle input, the microcontroller will provide the PWM signals to the gate drivers to drive the mosfets. The motor is controlled by the switching rate of the mosfets and transmits power through

<sup>15</sup> Section of circuit inside dotted line is the low power part of the circuit. The solid line indicates the high power part of the circuit. The mechanical system and power supply are outside of these lines.

the transmission system to the rear wheel. There are a number of sensors throughout the system that send updates to the microcontroller about the state of the system. These sensors can also directly influence the state of the system through additional circuitry we designed.

### Conclusion

At the conclusion of the project, we had accomplished full system integration physically. The major challenge remaining is creating a set of software that the microcontroller can use to control the system given all the feedback systems that communicate with it. Some additional features we may implement include creating a display and circuitry for monitoring the battery state. In conclusion, we have designed an electric hybrid bike with a minimal amount of additional weight, an integrated control system, based on the decision-making of the rider and microcontroller, and that is capable of greater efficiency than typical hybrid bikes through its use of regenerative motor control and various other feedback control mechanisms.

## Documentation and References

4QD-TEC: Electronics Circuits Reference Archive : PWM speed control <http://www.4qdtype.com/pwm-01.html>

[5] Brad Suppanz "Trace Width Calculator  
<http://www.geocities.com/CapeCanaveral/Lab/9643/TraceWidth.htm>

# **Appendix A:**

This appendix is a complete list of all the parts that we used in the project and their unit costs.

**Prices of Actual Parts Used**

Component	Manufacturer/ Dealer	Quantity	Total Part Cost (\$)
Printed Circuit Boards	APCircuits	2	175
IR2184 Gate Driver	Digikey	5	16.90
IR3709 Power Mosfets	Digikey	10	10.07
Fuses	Electrics Scooter parts	4	3.80
Fuse holders	Electrics Scooter parts	2	5.90
Amseco Magnetic Contacts (507-AMS-37B)	Mouser	1	5.63
Current sensing resistor CS3FR001-ND	Digikey	1	10.13
Current sensor 102-1069-ND	Digikey	1	20.75
SPDT Relays Siemens VF4	Digikey	1	3.96
VF4 Relay Socket	Digikey	1	1.51
SPST Switch	N/A	1	N/A
Resistors	N/A		N/A
Capacitors	N/A		N/A
1N914 High Speed Switching Diodes	N/A		N/A
15 V Zener Clamping Diode	N/A		N/A
TMP01 (Temperature Sensor)	Analog Devices	1	Sample
AD22057 Operational Amplifier	Analog Devices	1	Sample
PIC16F873A	N/A	1	N/A
4 Mhz Xtal Oscillator	N/A	1	N/A
LED's	N/A		N/A
Hall Effect Throttle	Electric Scooter Parts	1	19.95
Electromechanical brake lever	Electric Scooter Parts	1	14.95
HR15-12 Batteries	Electric Rider	2	73.48
Rad2go 24 VDC Scooter Motor	Electric Scooter Parts	1	100.85
#25 (5' chain)	Electric Scooter Parts	1	17.95
8MX-22S-12 Timing belt	Gates	1	N/A

Sprocket	Corporation		
8MX-67S-12 Timing Belt	Gates Corporation	1	N/A
I-5215-17 RMS Clutch Brake	Warner Electric	1	N/A
7858-0100 Taper Lock Bushing	Gates Corporation	1	N/A
7858-2600 Taper Lock Bushing	Gates Corporation	1	N/A
10 Gauge Wire	Mouser		N/A
#25 Sprocket (18 tooth)	Electric Scooter Parts	1	5.95
#25 rear Sprocket (55 tooth)	Electric Scooter Parts	1	19.95
<b>Total Costs</b>			<b>506.73</b>

### Component Sources

Alberta Circuits – <http://apcircuits.com/>

Digikey - <http://digikey.com/>

Electric Rider - <http://electricrider.com/>

Electric Scooter Parts - <http://electricscooterparts.com/>

Gates Corporation - <http://www.gates.com/index.cfm?CFID=3168568&CFTOKEN=80856193>

Mouser - <http://mouser.com/>

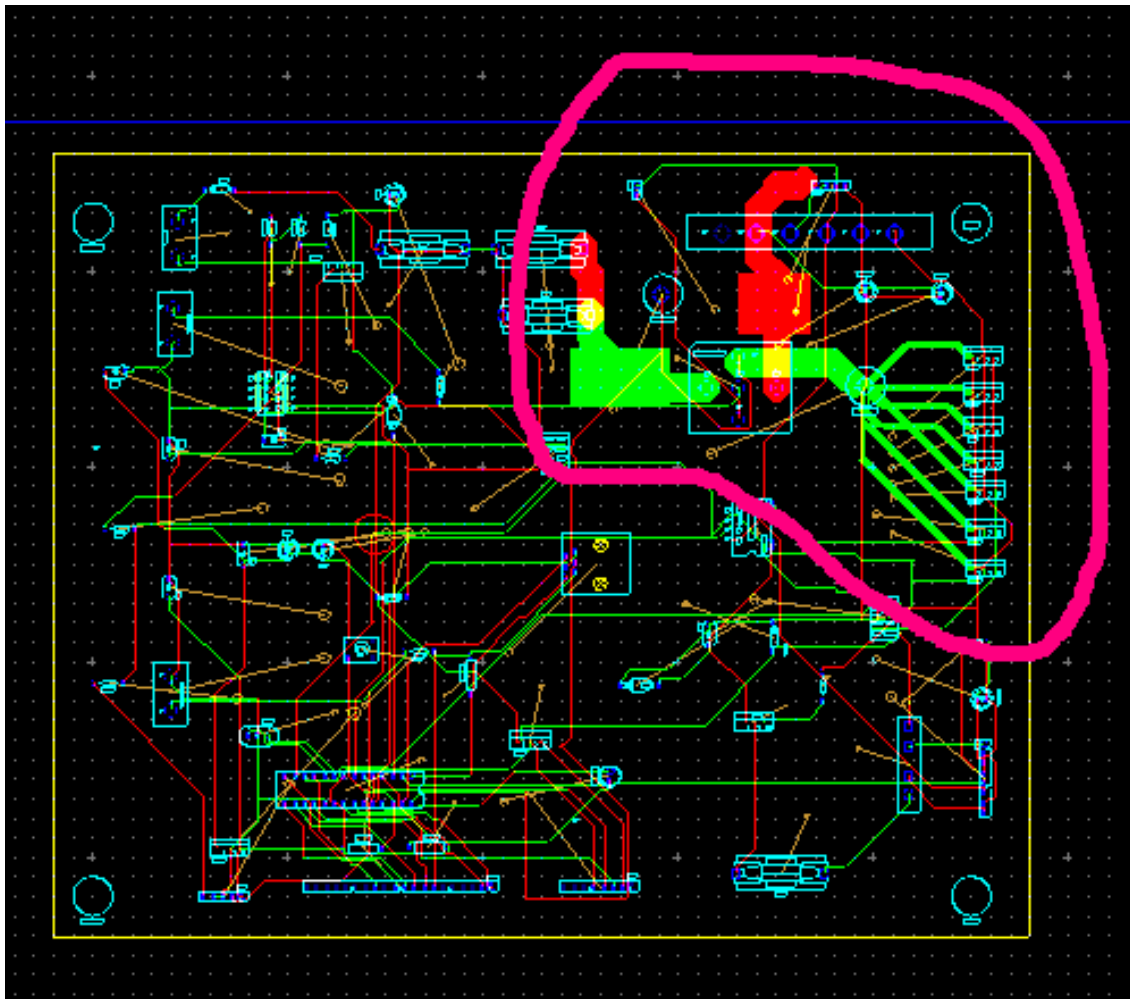
Warner Electric Corporation - <http://warnerelectric.com/>

# Appendix B:

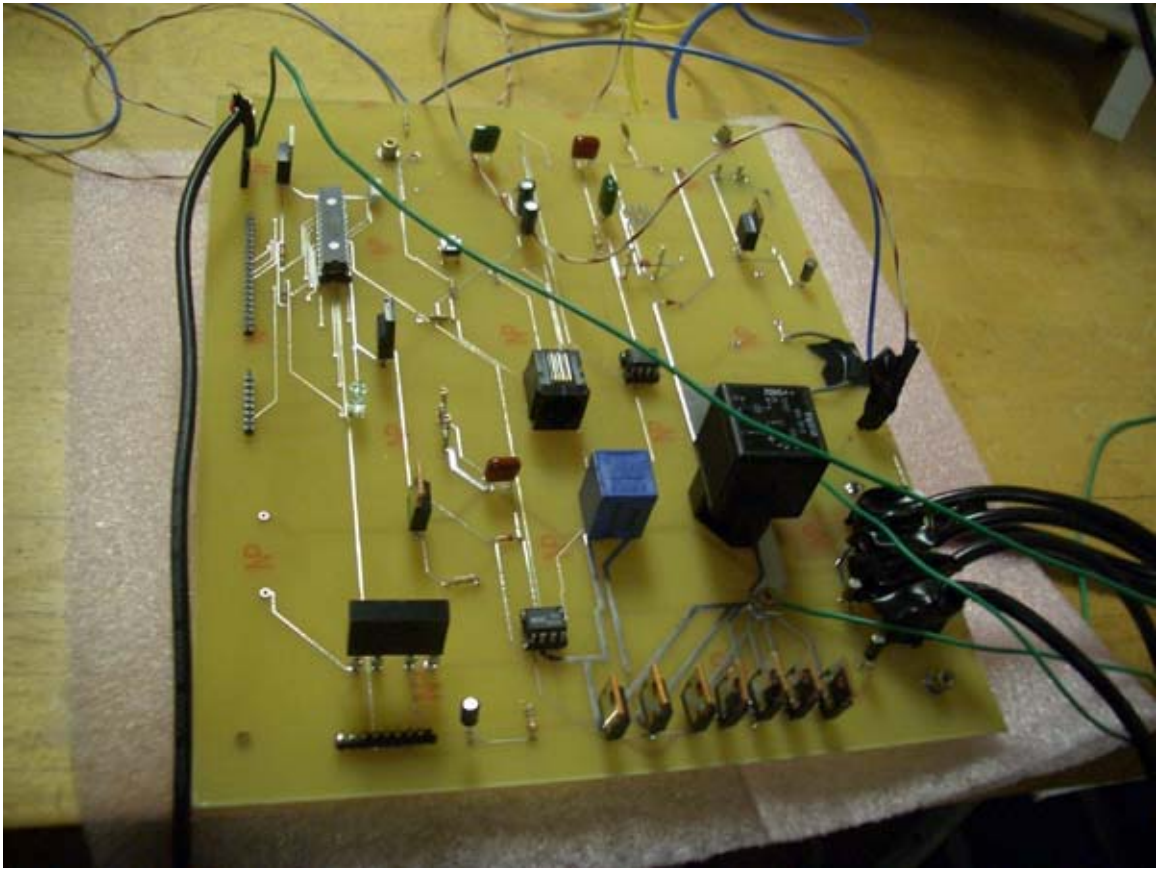
This section includes examples of the Multisim 7.0, Ultiboard 7.0 and physical circuit layouts.



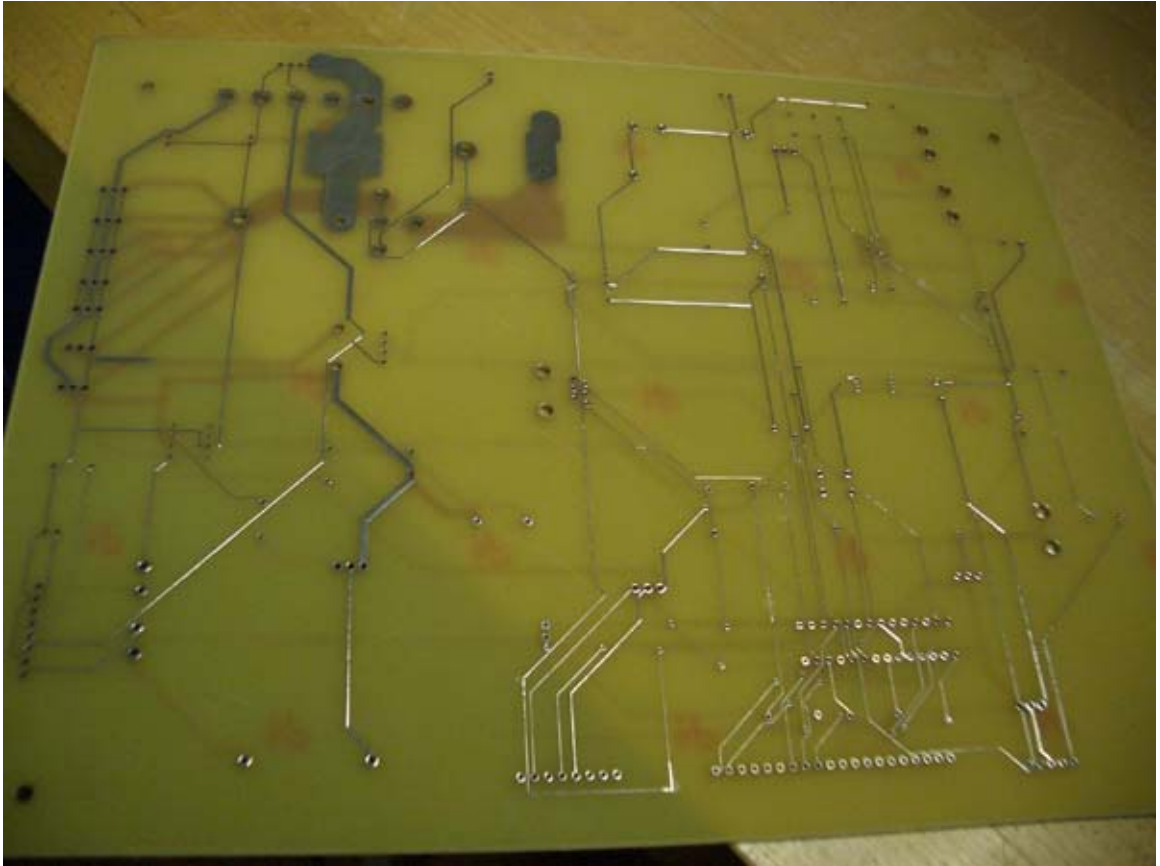
Ultiboard 7.0



PCB Controller Top Layer



PCB Controller Bottom Layer



# Appendix C:

This appendix includes sketches of the bike and power transmission system, the clutch and the detail report for the timing belt drive.

# **Appendix D:**

The following section includes pictures of the final system during and after mounting.

**Battery Mounts: Top and Bottom Plate**



**Motor Mount: Bottom and Side Plate**



**Timing Belt Pulley, Clutch and Jackshaft Mount**



**Complete Mounting System**



**Primary Drive Assembly**



**Complete Primary Drive and Power System**



**Rear view of Motor Assembly**

